Immaterial

Monolithic MOFs for Carbon Capture

CCUS Innovation 2.0

Final report

Feb 2025

Any enquiries regarding this publication should be sent to us at:
nzip@energysecurity.gov.uk

Contents

List of Figures

List of Tables

1. Executive Summary

The CCUS 2101 – Monolithic MOFs for Carbon Capture project, led by Immaterial, aimed to advance the development of monolithic metal-organic frameworks (m-MOFs) for carbon capture, utilization, and storage (CCUS) applications. The project successfully progressed the technology readiness level (TRL) from TRL 3 to TRL 4, demonstrating the feasibility of integrating monolithic MOFs into a pressure-vacuum swing adsorption (PVSA) system for efficient CO_2 capture from industrial flue gases.

Key Achievements:

Material Development and Optimization:

Three monolithic MOFs (IMM-16, IMM-16h, and IMM-28) were developed and optimized for CO_2 capture. These materials exhibited high CO_2 selectivity, mechanical stability, and resistance to humid conditions, making them suitable for industrial applications.

The synthesis process was scaled up from 10 mL to 30 L, maintaining material performance and achieving bulk densities between 0.8 and 1.4 g/cm³.

Process Design and Modelling:

A PVSA process model was designed, incorporating two generations of adsorption reactors (Gen.1 and Gen.2). The Gen.2 reactor demonstrated a significant improvement in productivity, achieving a capture capacity of 29 tonnes of CO_2 per tonne of MOF per year at 98% purity and 90% recovery.

Sensitivity analyses were conducted to optimize key process variables, including blowdown pressure, evacuation time, and bed porosity, ensuring efficient system performance.

Experimental Validation:

Cranfield University conducted extensive testing, including dynamic column breakthrough (DCB) experiments, thermogravimetric analysis (TGA), and material stability tests. These experiments validated the performance of the m-MOFs under various conditions, confirming their suitability for industrial deployment.

The project successfully demonstrated the materials' thermal, mechanical, and chemical stability, as well as their ability to maintain CO_2 adsorption capacity over multiple cycles.

Commercialization and Market Impact:

Immaterial engaged with key industry players across sectors such as cement, steel, and power generation, securing purchase orders and conducting feasibility studies. The techno-economic analysis highlighted significant cost savings compared to traditional amine-based capture technologies, with potential savings of €40-75 million annually for high CO_2 emitters.

A 5-year exploitation plan was developed, outlining the roadmap from pilot demonstrations to full-scale industrial deployment, with the aim of achieving commercial viability by 2029.

Intellectual Property Management:

Immaterial proactively protected its intellectual property, filing over 10 patents related to m-MOF chemistry, manufacturing processes, and carbon capture applications. The company also conducted extensive freedom-to-operate analyses to ensure the uniqueness of its technology in the market.

Conclusion:

The project successfully demonstrated the potential of monolithic MOFs for scalable and cost-effective carbon capture. By integrating advanced materials with optimized process designs, Immaterial has positioned itself as a leader in next-generation carbon capture technologies. The project's outcomes pave the way for further development and commercialization, with the next steps focusing on pilot demonstrations and industrial-scale validation. This progress aligns with global decarbonization goals and offers a promising solution for reducing CO_2 emissions from high-concentration industrial sources.

2. Project Outline, Aims and Objectives

The CCUS project was carried out to open a new route to the commercialisation of a low cost and scalable CO_2 capture technology based on monolithic MOFs. The objective was to deliver a demonstrator design that is validated at the fundamental level. The demonstrator unit will be built in a subsequent phase or in collaboration with our industry partners. In this project, the goal was to advance the TRL of our carbon capture technology from TRL 3 to 4 where our core technology of the engineered swing adsorption system integrated with monolithic MOFs is demonstrated. In doing so, the following specific tasks were planned:

- Improving structural stability of monolithic MOFs for conditions relevant to CO_2 capture from flue gas
- Morphology optimisation of monolithic MOFs for enhanced separation performance
- Engineering design of an energy-efficient PVSA system for rapid capture and release of CO_2
- Engineering design of a novel MOF-based structured adsorbent reactor for improved system performance
- Performance validation of a demonstrator design against data obtained from bench scale test rigs.

3. Roles and Contributions of Each Project Partner

Immaterial is the primary partner for this project, and no other partners are involved.

Cranfield University is the sole subcontractor for the project and leads Work Package 3 - Test rig adaptation and experimentation. Cranfield University is responsible for evaluating the performance of the optimised material developed in WP1 and validating and refining the process models built in WP2 using a bench-scale test rig.

4. Scope of Work and Results

4.1 WP1 - Material Selection and Optimisation

4.1.1 – Introduction

Flue gas CO_2 capture technologies aim to directly extract carbon dioxide from industrial exhaust gases, which typically contain CO_2 concentrations ranging from a 4 to 25 percent. Given the need for rapid and effective separation in high-throughput environments, these systems rely on materials with exceptional CO_2 affinity to enhance capture efficiency. Selecting the right materials can significantly impact the overall performance and energy demands of the capture process, making material choice a critical factor in optimising these technologies for sustainable, large-scale CO_2 capture.

Metal-organic frameworks (MOFs) are highly promising materials for carbon capture applications due to their exceptional porosity, tuneable structure, and high surface area. As they form with the assembly of metal clusters and organic ligands, they can

be designed to be used in a particular application. The ability to engineer the material in molecular level allows MOFs to selectively adsorb and store significant amounts of CO_2, even at low concentrations, making them ideal for efficiently capturing carbon from industrial emissions.

One bottleneck in the industrialisation of MOFs is the challenge of shaping them into a physical form suitable for deployment in industrial processes. MOFs are typically synthesised as powders, which are difficult to handle and integrate directly into carbon capture systems. To address this, MOFs need to be formed into stable structures, which is often achieved through pelletisation. However, pelletizing significantly reduces the accessible surface area of the MOF, which can cut CO_2 capture capacity by as much as half. This trade-off between structural stability and adsorption efficiency remains a key hurdle, underscoring the need for advanced shaping techniques that preserve MOF performance.

A second major bottleneck in the industrialisation of MOFs is the tough synthesis conditions required for these materials. Many MOFs are produced under specific, often challenging conditions involving high pressures and temperatures and toxic solvents. These requirements not only increase production complexity but also increase costs, making large-scale manufacturing difficult.

At Immaterial, we have tackled these key challenges in MOF shaping and scale-up by leveraging our innovative, green sol-gel technology to create densely packed monolithic MOF (m-MOF) particles with maximum capacity. This approach allows us to produce robust, high-performance m-MOF structures that retain the superior CO_2 capture efficiency of powdered MOFs while forming mechanically stable bodies of densely packed MOF nanoparticles. The result is a high volumetric capacity that meets the strict demands of industrial applications, providing both efficiency and structural integrity. Densely packed m-MOF beds will make a difference due to their high volumetric adsorption with the potential for a higher density of active material in the bed compared to other alternatives. Increased density allows for a greater amount of MOF material to be packed in a given volume leading to improved adsorption intensity, smaller equipment and footprint, and lower capital cost.

In this project, we chose three monolithic metal-organic frameworks (m-MOFs), namely IMM-16, IMM-16h, and IMM-28. IMM-16 and IMM-16h feature tetranuclear metal citrate clusters in an octahedral geometry, while the IMM-28 includes five-coordinated metal centres with a distorted trigonal bipyramidal geometry. (Figure 1) Each of these unique structures includes channels that selectively capture CO_2 over N_2, making it an outstanding candidate for efficient CO_2 capture from flue gases. Additionally, the materials' robust nature addresses stability issues commonly encountered by such materials in humid conditions, further enhancing their suitability for flue gas CO_2 capture.

Figure 1 - Schematic representation depicting the cluster geometry employed in the formation of IMM-16 and IMM-16h octahedral (a) and IMM-28 distorted trigonal bipyramidal (b).

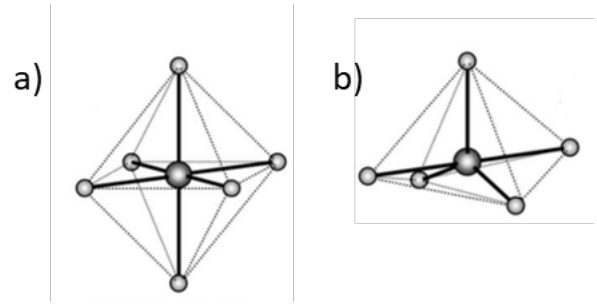

In order to develop a scalable recipe, it is necessary to adjust and optimize the synthesis conditions. The initial recipes outlined in the literature utilised substantial quantities of organic solvents. However, to minimise production costs at scale and to improve the safety and operability of the process with large-scale production, our goal has been to replace these solvents with water.

We have aimed to operate at the lowest practical temperatures (below 100°C) whenever feasible, thereby minimising energy costs on a larger scale and maximizing the efficiency of the process in terms of space-time yield. As a result, we explored different concentration levels to achieve the desired quality of the material at lower temperatures.

With all these optimisations described above we reached a product that demonstrates the anticipated adsorption performance as well as satisfactory density and mechanical stability. These optimisations were carried out at a synthesis scale of 10 ml, to produce approximately 1 g of material and achieve a bulk density ranging between 0.8 and 1.4 $g.cm^{-3}$.

4.1.2 – Characterisation Methods

CO_2 adsorption and desorption measurements were performed at room temperature using a Micromeritics 3Flex instrument (Figure 2).Prior to analysis, samples were degassed at 150 °C for 6 h under vacuum.

Figure 2: A picture of Micromeritics 3-Flex analyser.

Bulk density was obtained through EinScan-SE 3D Scanner. This technique was used to estimate the particle density of monoliths at atmospheric pressure by determining the volume. Prior to the analysis, all samples were activated overnight at 120 °C (vacuum) before measuring the mass.

Figure 3: A picture of EinScan-SE 3D scanner.

Mercury porosimetry was used also to measure the bulk density. Mercury porosimetry was obtained up to a final pressure of 4,000 bar using a POREMASTER-60 GT instrument from Quantachrome Instruments. Prior to the analysis, all samples were activated overnight at 120 °C (vacuum) before measuring the mass and then degassed in situ thoroughly before the mercury porosimetry.

Figure 4: A picture of the Hg porosimeter that are used for the analysis of the m-MOFs.

A vortex shaker was used to test the mechanical robustness of the produced monoliths. Scientific Industries SI™ Vortex-Genie™ 2 was used, with a speed range from 600 to 3200 rpm.

Figure 5: A picture of the vortex used for the mechanical testing of the m-MOFs.

Scanning electron microscopy (SEM) was performed using a FEI Nova NanoSEM at an acceleration voltage of 3.0 kV. Dried monoliths were prepared for analysis by crushing with a spatula and pressing a copper grid into the resulting powder. Images were processed with Image J software.

Breakthrough analysis has been conducted using an in-house-built test rig (see Figure 6) at 1 bar pressure using CO_2 and N_2 gas mixture at room temperature under dry and wet conditions. The design of a CO_2 capture adsorption system

requires an evaluation of the mass transfer kinetics of the adsorption mechanism which can strongly influence the process performance. To quantify the kinetic parameters, a lab-scale breakthrough test rig was constructed from Swagelok components to introduce a controlled gas mixture into a packed bed of MOF (approximately 5 g). On-line monitoring of the inlet flow rates of each component (using Bronkhorst MFCs), and the outlet CO_2 concentration (using an Alphasense NDIR sensor) produces a so-called “breakthrough curve”. The shape and gradient of the breakthrough curve are strongly influenced by the mass and heat transfer kinetics of the underlying system and material. Therefore, with appropriate material properties and equilibrium models, the kinetic parameters can be quantified through process simulations.

Figure 6: A picture of the in-house-built breakthrough rig.

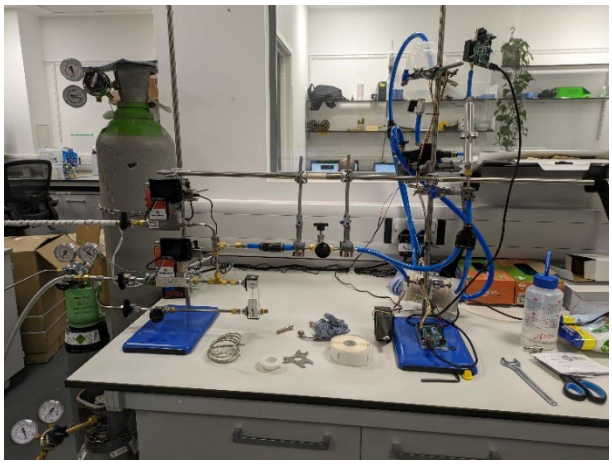

4.1.3 – Synthesis Optimisation

The synthesis process commenced with a solvent-water mixture as a solvent at a temperature below 100 Celsius. Subsequently, we optimise the solvent quantity and the concentration of the precursors. Through controlled adjustments, we successfully tailored the synthesis of the IMM-16 and IMM-28 crystals. This optimization resulted in the formation of a well-packed monolith with a high yield of up to 85% (Figure 7a), as opposed to the formation of a powdery pellet (Figure 7b).

Figure 7 (a) Photo of well particle-packed IMM-16 monoliths (b) Photo of powdery IMM-16 pellets.

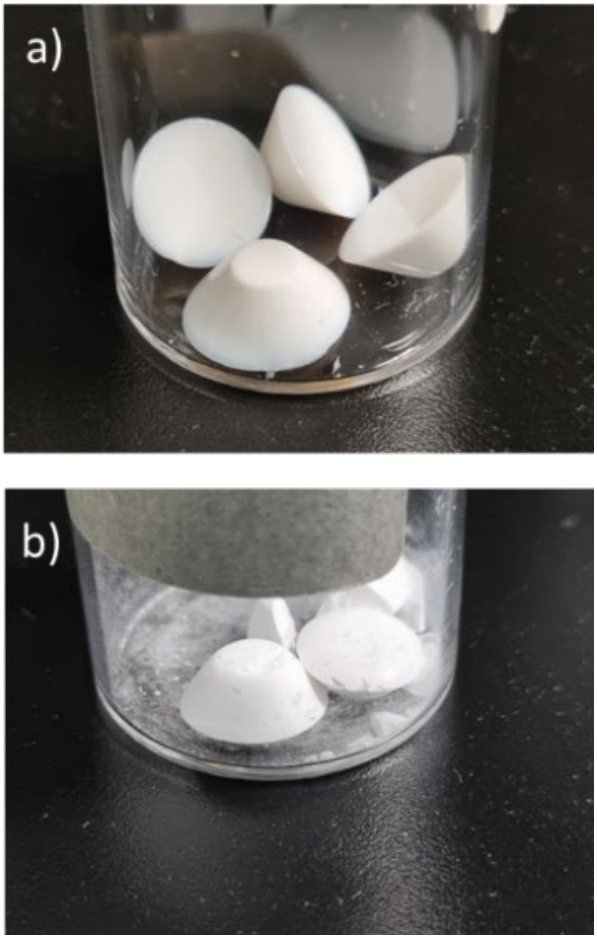

Then, the efforts focused on understanding the mechanical properties of the IMM-16 monoliths while preserving their adsorption capacity. To do that, a vortex shaker was used to test the mechanical robustness of the produced monoliths. The optimised monoliths were placed in a glass vial and vortexed at 3200 rpm for 10 seconds to test the robustness of the monoliths. We observed the pieces before and after to prove the robustness and measure the weight of the monoliths to quantify the loss of the material due to dusting caused by the vigorous shaking in a glass vial.

The vortex testing showed that we don’t have any disruption on the mechanical stability of IMM-16 after the treatment.

In order to enhance the performance of IMM-16 when exposed to humid streams, we proposed surface functionalization of the monoliths. Thus far, we have successfully observed the hydrophobic behaviour of the IMM-16h by simply adding water on top of the materials. (Figure 8)

Vortex testing of IMM-16h confirmed the mechanical stability of produced monoliths remain as the same after the hydrophobic treatment to create IMM-16h.(Figure 9a)

Figure 8 Pictures of IMM-16 (left) and IMM-16h (right) in contact of water. IMM-16h is repelling water when we drop water on the material.

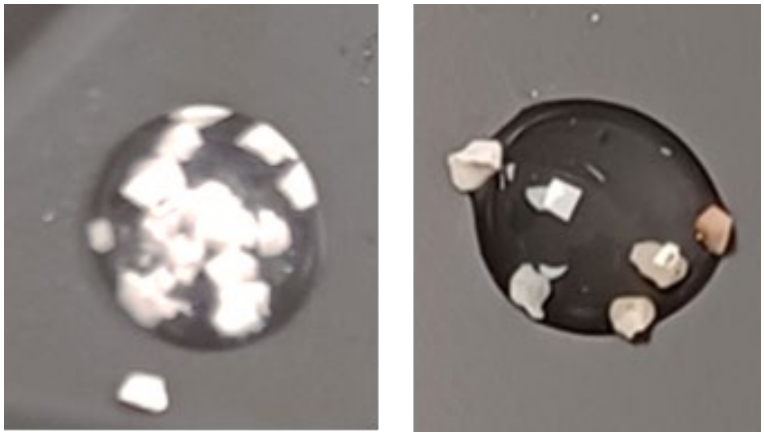

We used a very similar procedure in IMM-28 optimisation to achieve the desired mechanical stability where the produced monoliths had excellent CO_2 adsorption capacity (Figure 9b and Figure 10) as well as measured density of 1.3 $g.cm^{-3}$ for IMM-16 and IMM-16h, and 1.0 $g.cm^{-3}$ for IMM-28.

Figure 9 Picture of the vials after the vibration test on a IMM-16h monolith (b) and a IMM-28 monolith (b).

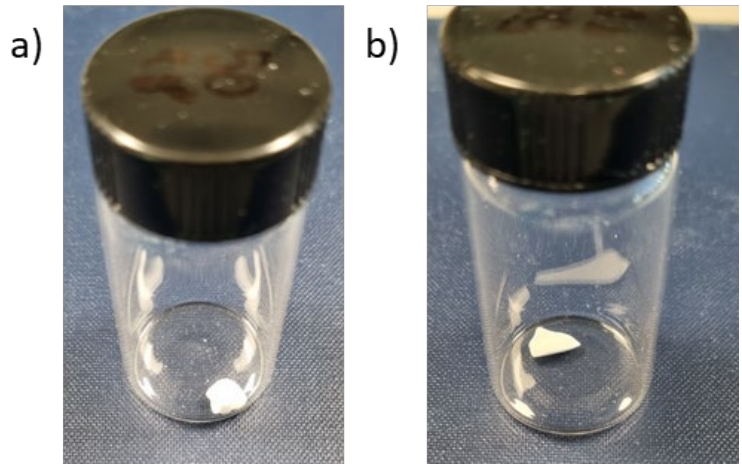

Scanning Electron Microscopy (SEM) images provided valuable insights into the characteristics of the nanoparticle size and the packing density of the particles within the monolithic structures. In our analysis, we focused on the optimized materials, specifically IMM-16 and IMM-28. As illustrated in Figure 10, the particle size for IMM-16 ranged from 500 to 550 nm, while IMM-28 exhibited a larger particle size, measuring between 900 and 950 nm. Additionally, the SEM images revealed the packing arrangement of these nanoparticles within the monoliths.

Figure 10 SEM images of monolithic IMM-16 (left) and IMM-28 (right)

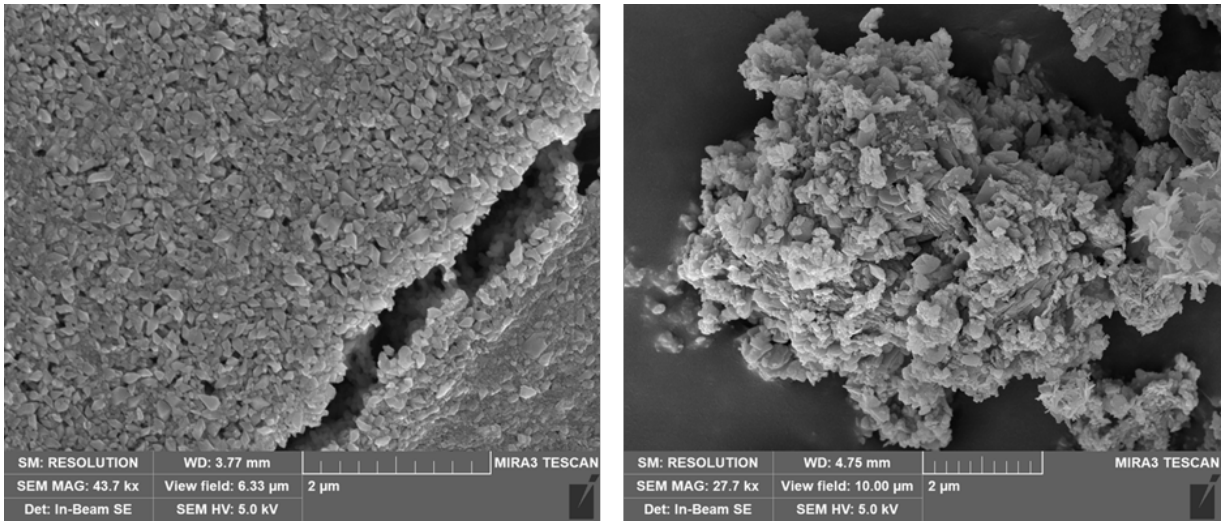

As a further characterisation for the particle packing, we measured the bulk density of the materials synthesised. The monoliths have been scanned through a 3-D scanner to determine the bulk volume. Monoliths exhibited a high density varying between 0.8 to 1.3 $g.cm^{-3}$. In the modelling, we used the density values obtained from 3D-scanner as we can do it quickly and accurately at Immaterial facilities. Then, we also measured macropore structure and the density of the optimised samples at University of Alicante in Spain through mercury porosimetry to compare the density calculation we have with another method. (Table 1) Although we have differences of approx. ±0.2 $g.cm^{-3}$, the trend between materials is the same regardless of different measurement techniques. We don't see any impact of this on the performance modelling compared to the data obtained by using 3D-scanner.

Table 1 Measured bulk density results were obtained by using a 3D scanner and Hg porosimeter.

	3D-scanner density ($g.cm^{-3}$)	Hg porosimetry density ($g.cm^{-3}$)
IMM-16	1.30	1.42
IMM-16h	1.24	1.05
IMM-28	1.0	0.8

Adsorption isotherms are fundamental for characterizing the m-MOF materials, given their microporous nature and significant applications in gas separation. We measured single-component isotherms for both CO_2 and N_2 at various temperatures to evaluate the selectivity of our materials for CO_2 over N_2, as well as to facilitate

calculations of the heat of adsorption. The results of these measurements are illustrated in Figure 11 providing critical insights into the performance and efficiency of our m-MOFs in capturing carbon dioxide.

Figure 11 Single component CO_2 and N_2 isotherms at different temperatures for IMM-16, IMM-16h and IMM-28.

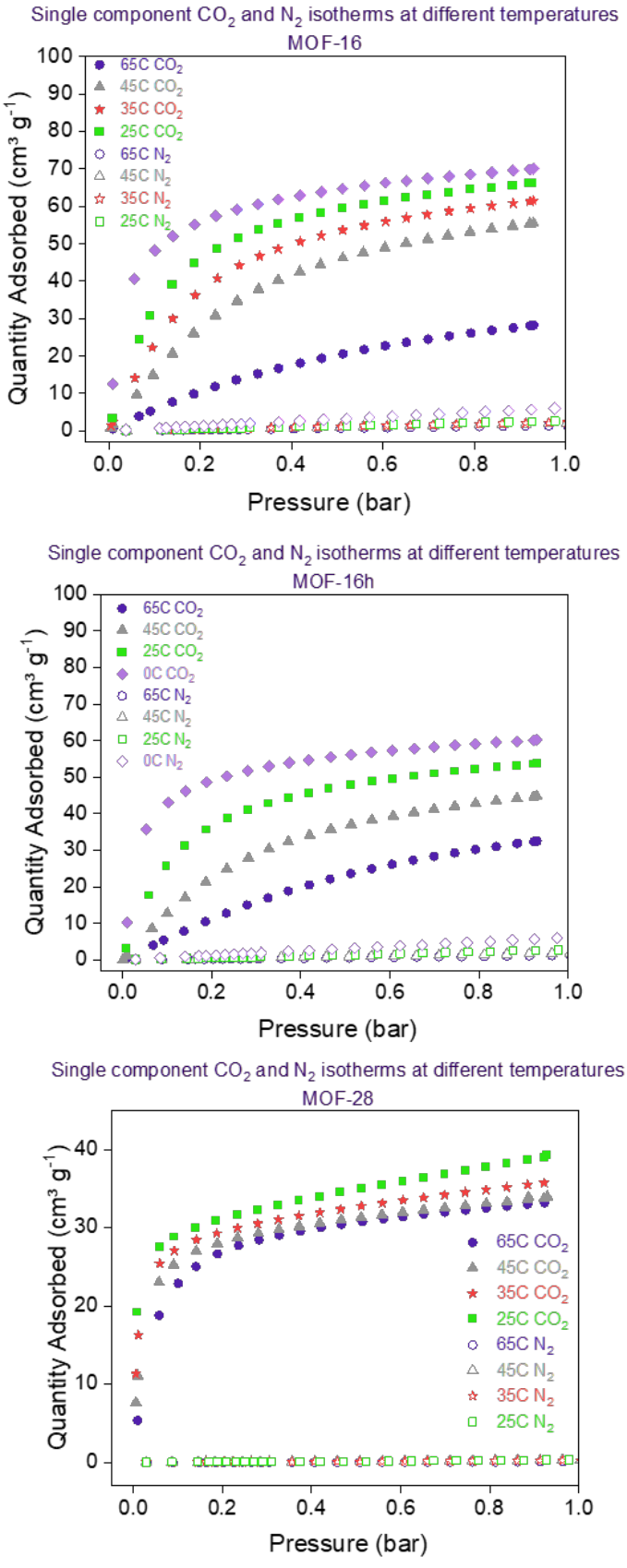

Breakthrough curves provide information about the kinetics of the gas adsorption. The breakthrough time specifically indicates details about convective mass transfer within the bed. The incline of the ascending curve discloses information about intra-particle macropore diffusions, while the region on the left-hand side of the curve typically signifies total gas uptake. In summary, comparing breakthrough curves for various gases yields valuable information regarding the competition among adsorbate molecules within the porous solid.

Initial analyses of breakthrough measurements for dry (CO_2 15% and N_2) and wet streams (CO_2 15%, N_2 and 50% RH) suggest insignificant mass transfer limitations . This behaviour is favourable for the dynamic of a typical VPSA process as it allows the system to achieve faster cycles and higher productivity.

To check the stability of our materials under moisture, we conducted single component CO_2 isotherm before and after the wet breakthrough testing. We conducted two cycles and performed the CO_2 adsorption analysis for all the samples. As evident from Figure 12, the three selected adsorbents show 5-10 % (IMM-16 and IMM-16h) or no loss (IMM-28) of capacity after being exposed to CO_2 streams with 50% relative humidity.

Figure 12 Single component CO_2 isotherms for IMM-16, IMM-16h and MOF 28 before and after exposure to moisture.

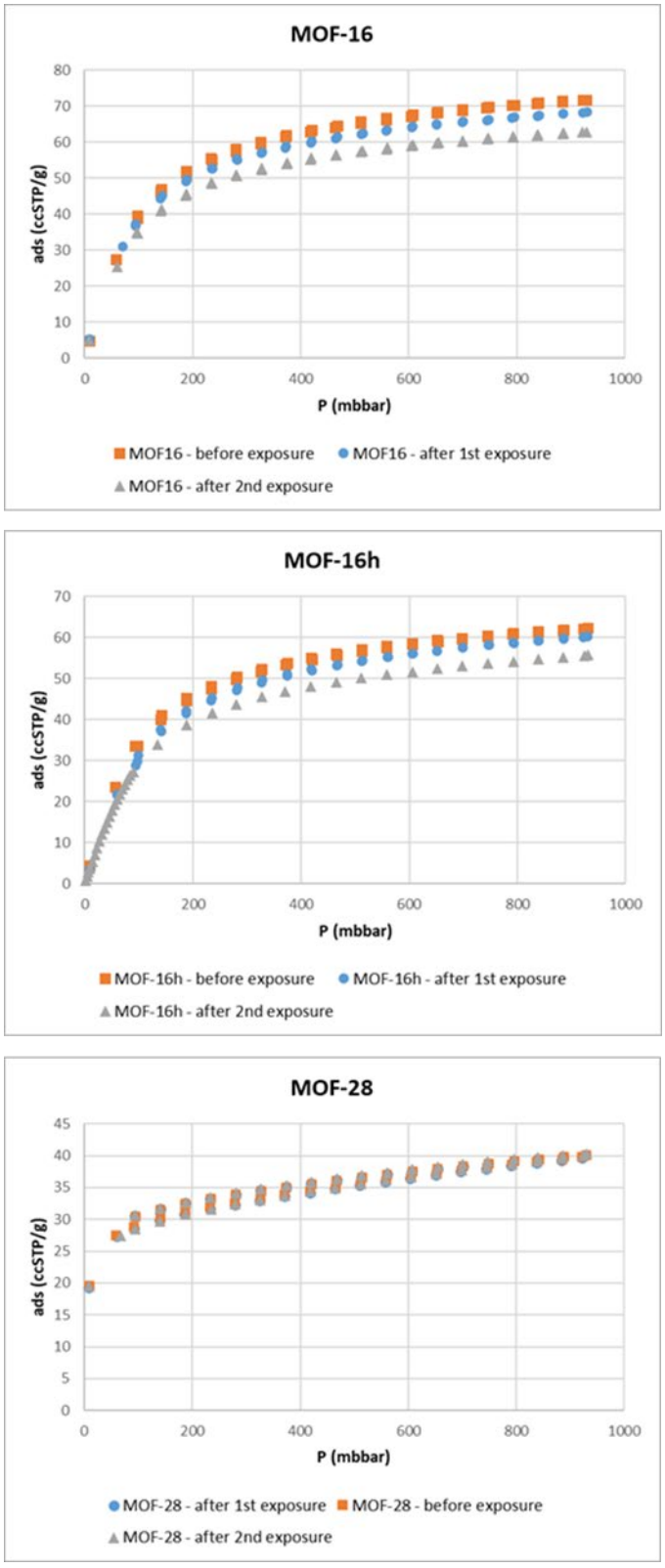

4.1.4 – Generation of Structured Adsorbents

As a further improvement, our second objective in this project is to utilize our m-MOF as shaped adsorbents, capitalizing on their enhanced volumetric capacity. This approach allows us to harness the inherent advantages that shaped adsorbents provide, such as reduced cycle times and improved kinetics in adsorption processes. Additionally, these m-MOFs help minimize pressure drops within the system, leading to more efficient operation. By achieving these objectives, we aim to significantly enhance the efficiency and effectiveness of adsorption systems, making them more viable for large-scale industrial applications and ultimately contributing to more sustainable carbon capture solutions.

We initially used the same formulations that had been developed for monolith production as a starting point in the expectation that they would need to be changed for a new application. The initial trials demonstrated this to be correct, and formulations need to be optimised for the particular shape. A notable challenge arose from their poor mechanical stability, leading to issues like cracking. Through iterative experimentation and refinement in the formulation, we successfully developed shaped bodies that showed improved mechanical stability.

We conducted multiple screenings, experimenting with the formulation of the sol-gel process. Among these trials, two different exemplar compositions represented by data points 97I and 97J in the plot in Figure 13 emerged as the optimal choice, offering superior mechanical stability while preserving the adsorption capabilities of the shaped m-IMM-16.

Figure 13 CO_2 adsorption isotherms at 21 °C of m-IMM-16 shaped adsorbents.

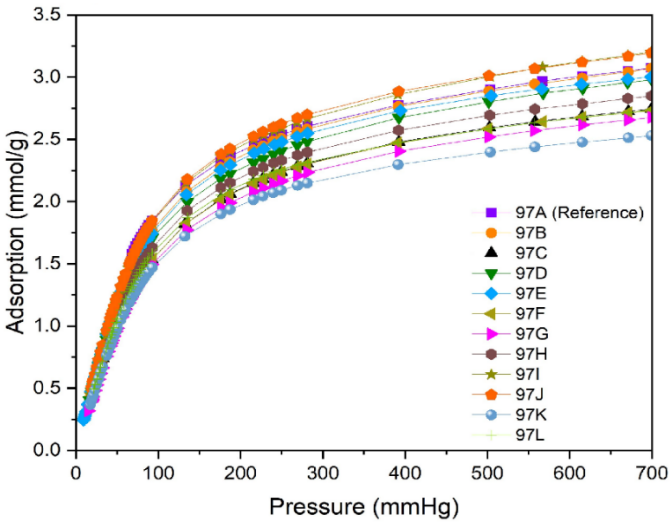

4.1.5 – Scale-up of the Optimised Procedures

After the successful small-scale optimisations of IMM-16 and IMM-28, we gradually started the scale-up production from 10 mL up to 30 L in 5 steps (50 mL, 200 mL, 1 L, 5 L and 30 L) to ensure the material maintains the same properties in each scale-up stage. The production process consists of four different steps: i) batch synthesis, ii) centrifuge washing, iii) drying, and iv) activation at 120 °C under vacuum. For 30 L batch reactions, we have used a large 30 L jacketed reactor with an overhead stirrer (Figure 14a). Heating is done by the oil circulating in the jacket around the reactor at a constant temperature. After the reaction, washing was done using a 750 mL centrifuge, and the materials were dried in the centrifuge buckets (Figure 14b). After drying the washed MOFs in the buckets, we end up with multi-centimetre size monolith bodies, which we carefully mill to the required particle size. 1.6 to 2 kg of the material can be achieved from a 30 L batch for both materials. Room temperature CO_2 adsorption isotherm of the two samples synthesised in 30 L batch size exhibited a similar CO_2 uptake with compared to small batches. (Figure 15).

Figure 14 Photos of a large-scale (30 L) reaction (a). MOFs drying in the buckets to produce monoliths. (b)

a)

b)

Figure 15 CO_2 isotherms at room temperature for the products produced by different batch size. IMM-16 (a) and IMM-28 (b)

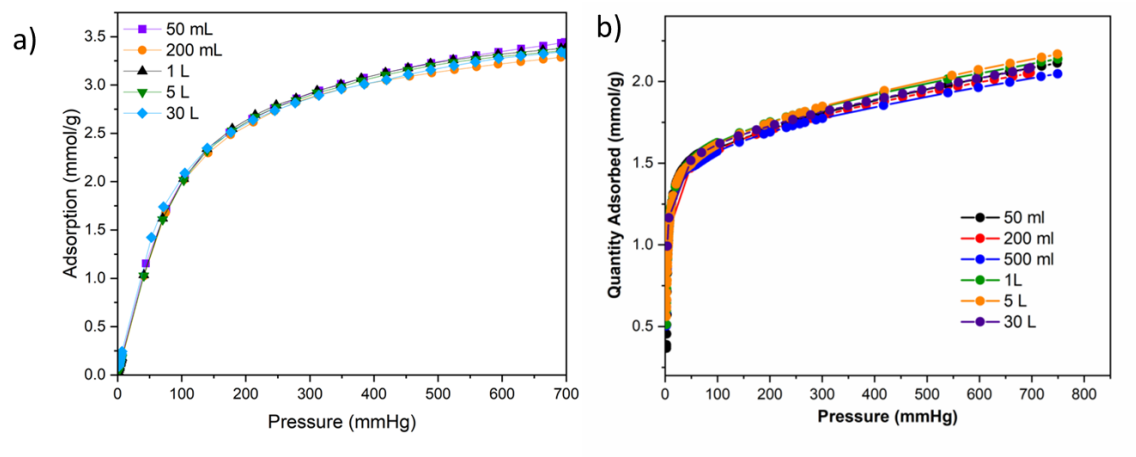

After drying the washed MOFs in the buckets, we end up with multi centimetre size monolithic cakes (Figure 16a). These cakes are highly dense and porous materials ready to be chopped down to any particle size needed by the application. The density measured through the 3D scanner produced by 30 L batch reactor were measured as 1.24 $g.cm^{-3}$ for IMM-16 and IMM-16h, and 1.06 $g.cm^{-3}$ IMM-28 are in agreement with the small scale.

Figure 16 Multi-centimetre sized monolithic IMM-28 cakes (a) and chopped IMM-16 samples to a specific particle sizes (b).

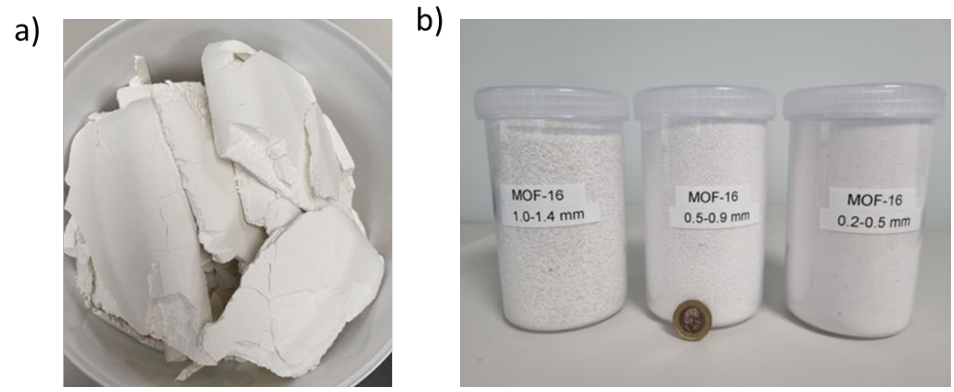

Optimizing particle size in adsorption systems will critically affect balancing the trade-offs between adsorption kinetics and pressure drop. Smaller particles typically offer faster adsorption kinetics due to their larger surface area-to-volume ratio, but they also result in higher pressure drop due to increased resistance to flow. Conversely, larger particles reduce pressure drop but may exhibit slower adsorption kinetics. By systematically investigating the relationship between particle size, adsorption kinetics, and pressure drop, we aim to identify the optimal particle size range that maximizes adsorption efficiency while minimizing energy penalties in our adsorption system.

4.2 WP2 - Design of a PVSA Process Model

4.2.1 – Introduction

Work Package 2 of the CCUS project (WP2) is dedicated to engineering design and optimisation of a scalable CO_2 capture system that can be retrofitted to existing “high concentration” (i.e., ≥15%) point sources of flue gas such as coal-fired power plants, cement and steel factories. In this context, WP2 aims to develop a novel adsorption-based process system using two different generations of adsorption reactors (Gen.1 and Gen.2) which are tuned for operation of Immaterial’s proprietary monolithic metal-organic frameworks (m-MOFs). The system can recover CO_2 from feed streams and concentrate it with ≥96% purity, while at the same time maximising productivity of the process. As part of the above objectives, WP2 obtains and analyses important technical information regarding cycle configurations, and key performance indicators (KPIs) of the designed process for a given set of operating conditions. The engineering knowledge obtained from this work package will be crucial for the detailed design and building of a demonstrator unit that can be commissioned in collaboration with our industry partners in a separate phase of the project.

4.2.2 – Adsorbent Selection and Choice of the Process Cycle

The first step in design of an adsorption-based carbon capture system is the choice of an appropriate process cycle based on properties of available adsorbents, and conditions of the flue gas. For this purpose, we considered adsorption behaviour of Immaterial’s top 3 adsorbent materials, namely IMM-16, IMM-16h, and IMM-28 whose synthesis and material properties are described in separate deliverable reports for WP1 and WP3. Equilibrium adsorption isotherms of these materials for CO_2 and N_2 (two major components of the flue gas) are shown in Figure 17. As evident from this figure, IMM-16 appears to have the desired characteristics of an ideal adsorbent for CO_2 capture in terms of total uptake, shape, Henry’s law constant, and selectivity over N_2. The next step in the design of an adsorption separation system is associated with the choice of an appropriate process cycle that can realize maximum potential of the selected adsorbent. For this, we have designed a pressure-vacuum swing adsorption (PVSA) process using two generations of reactor beds that are optimized based on adsorption characteristics of Immaterial’s IMM-16 adsorbent.

Figure 17. Single-component adsorption isotherms of CO_2 and N_2 for IMM-16, IMM-16h and IMM-28

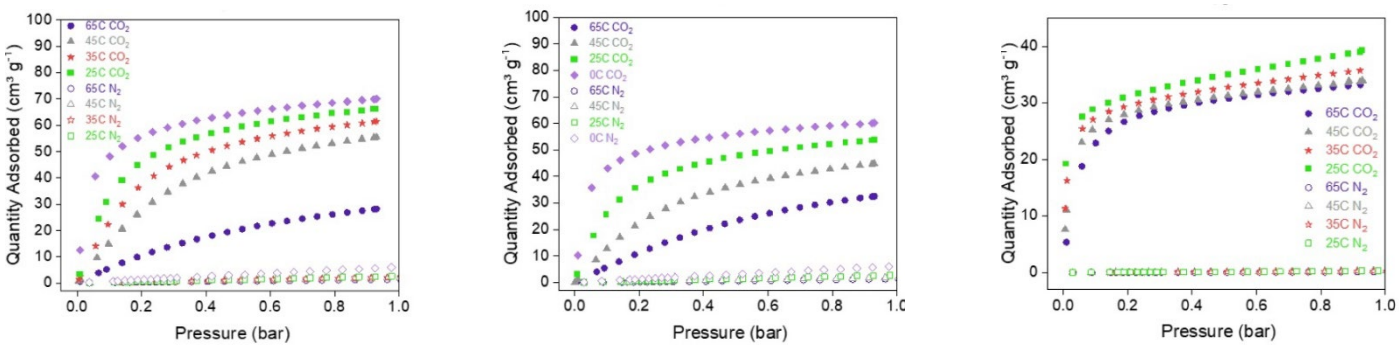

4.2.3 – System Engineering Design of the DR-VPSA Process

Model Construction

Modelling and optimization of the PVSA process constitute two major activities of WP2 which are preceded by a series of prerequisite tasks including collation of physical property data, numerical modelling of adsorption equilibrium data, bed engineering, and cycle scheduling.

Collation of Physical Property Data

Process modelling of swing adsorption systems require a large set of input data and parameters that are either obtained from experimental measurements or established through available theories. The most important set of data required for process modelling and optimization of PVSA systems include bed porosity, bed dimensions and geometry, pellet density, pellet heat capacity and thermal conductivity, equilibrium gas adsorption and isosteric heat of adsorption data for all components of the feed; mass transfer coefficients associated with intraparticle diffusion of adsorbate molecules, and fluid heat capacity and thermal conductivity. These parameters are measured experimentally as presented in different chapters of this report.

Numerical Fitting of Equilibrium Adsorption Data

Equilibrium adsorption isotherms of two main components of dry feed (CO_2 and N_2) are measured experimentally up to 1 bar at different temperatures (Figure 17). Isotherms with temperatures relevant to operating conditions of the process were then fitted to an appropriate numerical adsorption model so that they can be used by our process modelling tool for interpolation of the data as required. We have fitted sub-atmospheric experimental adsorption isotherms of CO_2 and N_2 at 3 different temperatures using a dual-site Langmuir adsorption (DSL) model, results of which are presented in Figure 13. The DSL model as described by eq. (1) is a powerful tool

for correlating multicomponent gas adsorption data to single-component adsorption isotherms.

$$q_i^* = \sum_{j=1}^{2} \left[q_{j,i}^s \frac{b_{j,i} P}{1 + b_{j,i} P} \right] \qquad \text{eq. (1)}$$

In this equation, q_i^* denotes total gas uptake, $q_{j,i}$ is saturation capacity of site j with respect to species i, and $b_{j,i}$ describes affinity of each site. The DSL model has been shown to be a simple and yet adequate model for fitting type-I adsorption isotherms of simple gases such as CO_2, N_2, and O2 which has been widely adopted by the scientific community for modelling adsorption processes in the context of carbon capture[1].

Figure 18. Experimental (black) and DSL-fitted (red) adsorption isotherms of CO_2 and N_2 in IMM-16 at 4 different temperatures of 273 K, 298 K, 318 K, and 338 K. The isotherms appear in descending order from top to bottom as 273 K, 298 K, 318 K, and 338 K

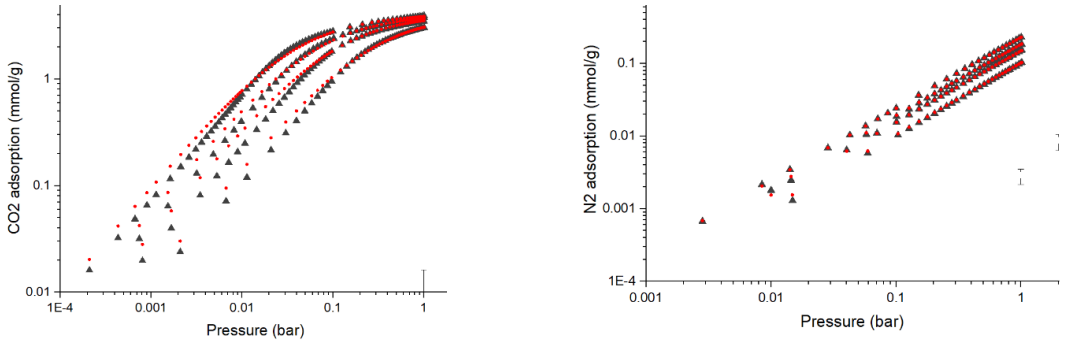

From Figure 18, it is evident that the DSL model (red symbols) can provide an accurate fitting of the experimental data (black symbols) within the pressure range of interest.

Gen. 1 Reactor Design

Sizing of the reactor is the main part of bed engineering. This is where maximum theoretical capacity and footprint of the process system is determined. The other important aspect of bed engineering is related to defining physical limitations of the bed in terms of the amount of feed flow that can be processed without fluidizing the bed. In our Gen.1 design, total volume of the reactor is $0.75\ m^3$ $(L = 1.5\ \ m, D = 0.8\ m)$ with aspect ratio of $\frac{L}{D} = 1.875$. The reactor diameter was determined based on the required feed flowrate while ensuring the gas velocity remained below the fluidization threshold. The aspect ratio of $\frac{L}{D}$ was influenced by the dimensions of the

[1] Ind. Eng. Chem. Res. 2018, 57, 45, 15491–15511

container designated to house the bed. Further details of the reactor bed are provided in Table 2.

Table 2. Physical properties of Gen.1 adsorption reactor

Pellet diameter	Pellet density	Pellet porosity	Bed density	Bed porosity	Bed length	Bed diameter	Bed volume	Minimum fluidization velocity	Porosity at fluidization
3 $(\boldsymbol{mm})$	1240 $(\frac{kg}{m^3})$	0.23 $(-)$	744 $(\frac{kg}{m^3})$	0.4 $(-)$	1.5 (m)	0.8 (m)	0.75 (m^3)	0.52 $(\frac{m}{s})$	0.415 $(-)$

It should be noted that we have designed our system for feed streams containing 15% CO_2 and 85% N_2 on dry basis with total flowrate of 1642 kg/hr. There are normally small mole fractions of other gas components in the feed including water vapour, oxygen, SOx, NOx and various particulates depending on the feed source. Our assumption for using a binary feed mixture consisting of CO_2/N_2 is valid because with exception of oxygen, all other components will be removed from the feed using pre-treatment units located upstream of the carbon capture system, consistent with industrial practice for flue gas conditioning[2]. Pre-treatment units such as dehumidifiers or SOx and NOx scrubbers are standard unit operations that are commercially available, and their design is outside the scope of the current project. As for oxygen, adsorption behaviour of this component is known to be similar to that of nitrogen; hence its mole fraction in the feed is combined with that of N_2 in our modelling study.

The design provided in this section results in a system with an insignificant pressure drop (i.e., 1.8 kPa) across the bed for the given flowrate of the feed. This is a favourable figure because low pressure-drops would allow a non-energy intensive PVSA process to be constructed for the system of interest. The pressure-drop profiles of the bed versus superficial velocity, and flowrate of the feed are illustrated in Figure 19.

[2] IPCC Special Report on Carbon Dioxide Capture and Storage (2005)

Figure 19. Pressure-drop across the bed with respect to superficial gas velocity and flow rate of the feed

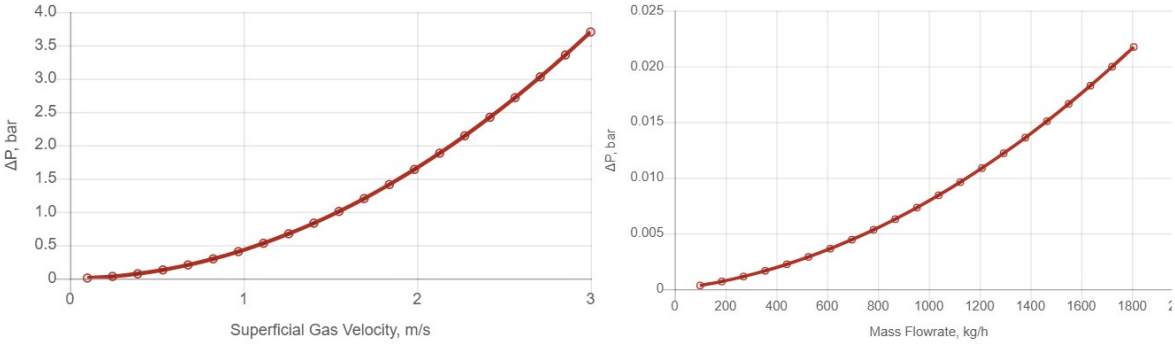

Cycle Design

We have considered various process configurations and compared them with those already reported in the literature. Having reviewed different aspects of these processes, we ultimately designed a new PVSA cycle which was later optimized based on Immaterial's top-performing m-MOFs. The proposed PVSA cycle consists of several consecutive steps from which only the typical steps are described below:

Adsorption or feeding step: At this step the reactor is exposed to feed during which CO_2 is selectively adsorbed by m-MOF, while N_2 leaves the bed as effluent from the product end of the reactor.

Blowdown: Pressure is reduced during Bd to intermediate pressures in order to remove N_2 from the bed, hence improving purity of CO_2 in the subsequent evacuation step.

Evacuation: This is when pressure of the bed is reduced even further using a vacuum pump to collect concentrated CO_2 as product.

Re-pressurization: the bed is repressurized after the evacuation up to the level required for the start of adsorption step in the next cycle.

To simulate performance of the PVSA cycle, a process model was developed where each of the cycle steps are explicitly implemented.

Cycle Scheduling

PVSA cycles often require multiple reactor beds to achieve the desired separation. At the same time, to maximize productivity of the carbon capture plant, it is preferred to construct a system with continuous flow, meaning at any given time at least one of the reactor beds should undergo a feeding step. To allow continuous feeding of the system, while matching relevant flow streams between interacting beds, a careful cycle schedule must be designed. The minimum number of columns required to

implement the cycle in this way is called a “train”. It should be emphasized that the above train constitutes the most fundamental unit of our carbon capture system. For large-scale commercial plants, parallel trains must be simultaneously utilized to handle large flowrates of the feed. The design of a multi-train capture plant is outside the scope of the current demonstrator design.

Dynamic Behaviour and Optimization of the System with Gen.1 Reactor

To fully understand dynamic behaviour of the system, an extensive set of breakthrough measurements are required. These measurements will provide crucial information about breakthrough time and mass transfer limitations of adsorbent material which will be then used to adjust duration of different steps and estimate mass transfer coefficients of CO_2 and N_2. These measurements are carried out as part of WP3.

Process optimization is generally a challenging task for multi-steps PVSA cycles where a large set of decision variables contributes to overall performance of the system. Here, purity and recovery of CO_2 are defined by eq. (2) and eq. (3) which must be simultaneously maximized during the optimization process.

$$\text{purity} = \frac{\text{total mol } CO_2 \text{ in extract product}}{\text{total mol } CO_2 \text{ and } N_2 \text{ in extract product}} \times 100 \qquad \text{eq. (2)}$$

$$\text{recovery} = \frac{\text{total mol } CO_2 \text{in extract product}}{\text{total mol } CO_2 \text{fed into cycle}} \times 100 \qquad \text{eq. (3)}$$

Eleven decision variables are considered in our process optimization resulting in a highly multi-dimensional optimization space. These variables include duration of all steps; various stream flowrates; as well as blowdown and evacuation pressures. Figure 15 illustrates the outcomes of a number of different optimization trials with respect to purity and recovery of the PVSA process. The chosen cycle schedule also adds an additional constraint on duration of each step; hence only configurations that satisfy these constraints can be accepted. The best purity and recovery of CO_2 (purity = 96%, recovery = 86%) for the chosen cycle schedule is shown by a blue diamond symbol in

Figure 20. Evidently, the CO_2 product captured by our carbon capture unit meets the 96% minimum purity specification of the transfer and storage (T&S) infrastructure as defined in the CCUS Innovation 2.0 call.

Figure 20. Purity and recovery of the PVSA cycle for different optimization trials. Best configuration fulfilling the cycle schedule is shown by a blue diamond symbol.

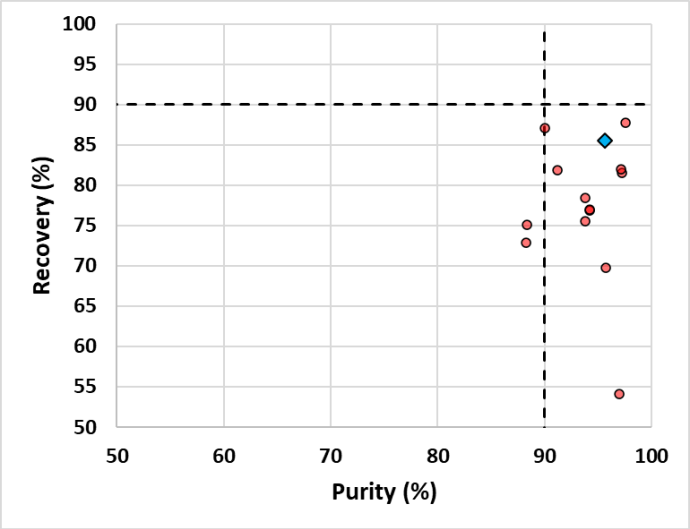

Another important KPI in the design and optimization of separation processes is productivity of the process as described by the following equation:

$$\text{productivity} = \frac{\text{total mol } CO_2 \text{ in extract product}}{(\text{total volume of adsorbent}) \times (\text{cycle time})} \qquad \text{eq. (4)}$$

Currently, for the given process configuration with purity = 96% and recovery = 86%, productivity of the Gen.1 demonstrator train is 7.32 $\frac{tonne\ of\ CO2}{day}$. On annual basis, a single CO_2 capture unit designed in this work will be able to capture 2,670 tonne of CO_2 which will require 1.68 tonne of IMM-16.

Development of Gen. 2 Reactors

The original application submitted for the “CCUS Innovation 2.0 Call” proposed the development of a carbon capture system using two different reactor designs namely Generation 1 and Generation 2. Engineering design of the Gen. 1 system was explained in the previous section, while design of the Gen. 2 reactor is subject of the present section. For the Gen. 2 reactor, the primary goal is to increase process productivity through design of faster cycles. At the same time, the new design aims to reduce overall energy consumption of the process by minimizing pressure drop across the bed.

The use of Gen. 2 reactors allows processing a significantly larger volume of flue gas with smaller pressure drop and reduced mass transfer resistance. This generation of reactor incorporates equally spaced parallel passages that allow for higher gas velocities without fluidization, while also enhancing mass transfer kinetics. These

considerations form the basis of our Gen. 2 reactor design which is meant to be incorporated into a compact rapid-cycle PVSA system.

Dynamic Behaviour and Optimization of the System with Gen. 2 Reactor

The Gen. 2 adsorption reactor is designed based on Immaterial's proprietary structured adsorbent form factor where heat and mass transfer properties of adsorbents are significantly improved compared to pelletized m-MOFs. Gen.2 reactor design is used to enhance process productivity through the implementation of rapid cycles. At the same time, the new design reduces overall energy consumption of the process by minimizing pressure drop across the beds. Table 3 summarizes physical properties of the Gen. 2 reactor designed in this work.

Table 3. Physical properties of Gen. 2 adsorption reactor

Bed density	Bed porosity	Bed length	Bed diameter	Bed volume	Pressure drop
100 - 170 $(\frac{\boldsymbol{kg}}{\boldsymbol{m^3}})$	0.7 – 0.8 $(-)$	1.5 (m)	0.8 (m)	0.75 (m^3)	2 - 5 $(mbar)$

To better understand adsorption kinetic of CO_2 and N_2 gas mixtures in Gen.1 and Gen. 2 reactors of m-MOFs, we have conducted a detailed analysis of relevant gas diffusivities which include estimation of Knudsen and molecular diffusivities along with macropore, effective macropore, and effective pellet diffusivities. Here, the goal is to estimate mass transfer coefficients (MTC) of CO_2 and N_2 as obtained from the linear driving force (LDF) model. The results from these analyses suggest that mass transfer rates estimated using LDF model are >400 times larger in our Gen. 2 adsorbents compared to those associated with Gen.1 MOFs.

To intensify our PVSA cycle, a suitably sized Gen. 2 reactor was incorporated into the process. The new reactor contains 127 kg of IMM-16 in different form factors. By capitalizing on rapid mass transfer kinetic of CO_2 and N_2 in structured forms of IMM-16, we were able to increase feed flow rate by a factor of 4, while simultaneously reducing total cycle time. Significantly faster mass transfer improved bed utilization through sharpening of adsorbed-phase CO_2 front in the reactor.

In our Gen. 2 reactor, we were able to increase feed flowrate of the system by a factor of 4 without increasing bed dimensions which suggests a shorter residence time is achievable. A shorter residence time allows us to reduce duration of adsorption step without any CO_2 breaking through from the bed. This observation is shown in Figure 21 where adsorbed-phase profiles of Gen.1 and Gen.2 reactors are compared. It should be noted that in this figure the Gen.1 reactor has been on feed

for 100 seconds (left figure), however, for the system with Gen. 2. design, the feeding time is reduced to 25 seconds!

Figure 21. Comparison of adsorbed-phase front in Gen. 1 (left) and Gen. 2 (right) adsorption reactors. Blue and red curves represent CO_2 and N_2 concentrations respectively.

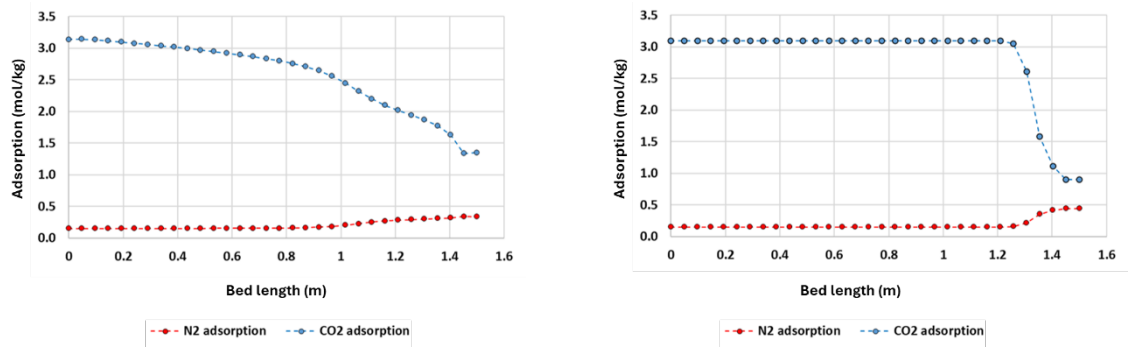

To achieve maximum productivity, we have intensified performance of our PVSA cycle through incorporation and optimization of our Gen. 2 reactor. The intensified cycle shows a dramatic increase in gravimetric productivity (by a factor of 18) which is the result of simultaneous improvement on multiple fronts including increased feed flowrate, reduced cycle time, enhanced mass transfer, and higher bed utilization. The intensified PVSA unit is now capable of capturing 29 $\frac{\text{kte CO2}}{\text{te MOF.year}}$ at 98% purity and 90% recovery meeting the scales required for building a commercial CO_2 capture plant. Figure 22 compares the results of process optimization for Gen.1 and Gen. 2 PVSA systems.

Figure 22. Comparison of system's performance between Gen.1 (red symbols) and Gen.2 (blue symbols) designs.

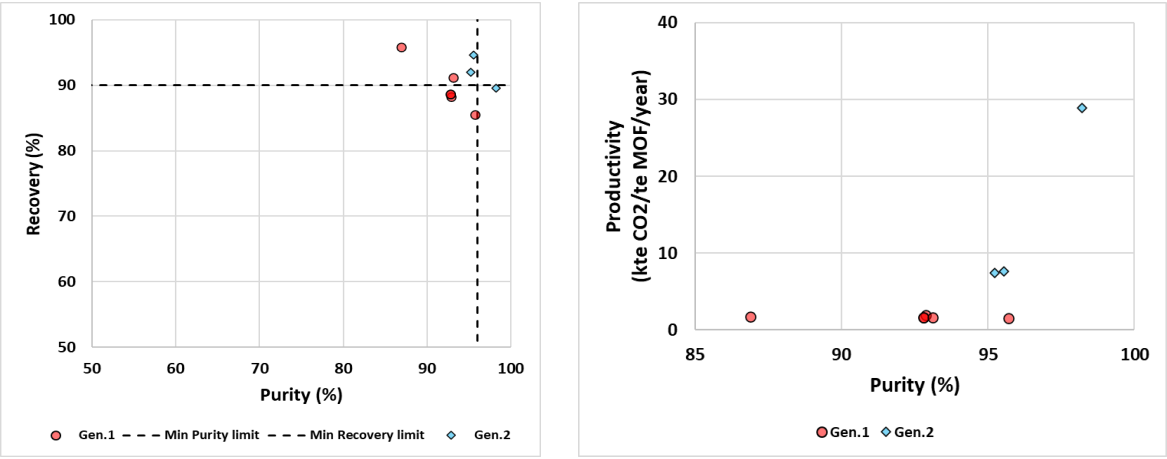

4.2.4 – Sensitivity Analysis of the PVSA Process

This section is dedicated to sensitivity analysis of the PVSA system. Here, we report on the outcome of a series of sensitivity analyses carried out to better understand the complex interplay between different process variables and their collective or individual impacts on overall system's performance.

Understanding the Impact of Blow-down and Evacuation Steps

N_2 and CO_2 products are produced during blow-down (Bd) and evacuation (Evac) steps of the process. Bd and Evac pressures along with duration of each step dictate purity of N_2 and CO_2 products respectively. We performed sensitivity analysis to understand the impact of these cycle variables on purity and recovery of the system, the results of which are shown in Figure 23.

Figure 23. Variation of CO_2 purity and recovery with respect to blow-down pressure

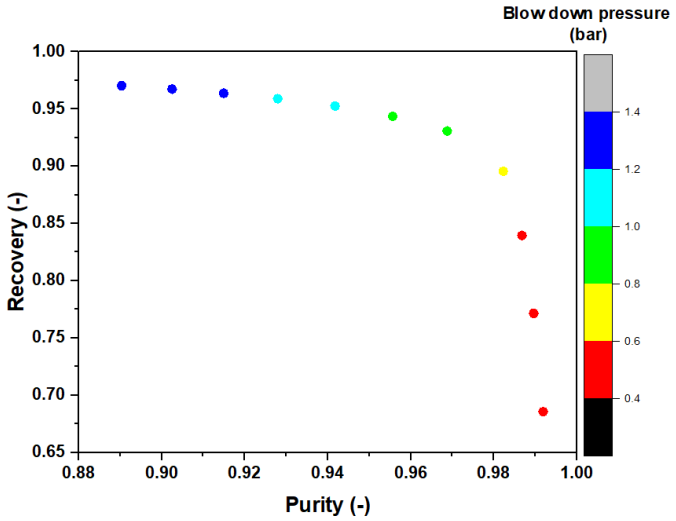

As demonstrated by this figure, CO_2 purity is enhanced at lower blow-down pressures due to N_2 being almost completely removed from the product stream before the evacuation step. Lower blow-down pressures, however, result in lower CO_2 recoveries considering CO_2 starts to desorb at these pressures and hence leaving the bed along with N_2. This analysis also suggests the optimum value of blow-down pressure to be around 0.76 bar.

Another set of sensitivity analyses focused on the impact of blow-down and evacuation step times on purity and recovery of CO_2, with their corresponding results illustrated in Figure 24.

Figure 24. Variation of CO_2 purity and recovery with respect to duration of blow down and evacuation steps

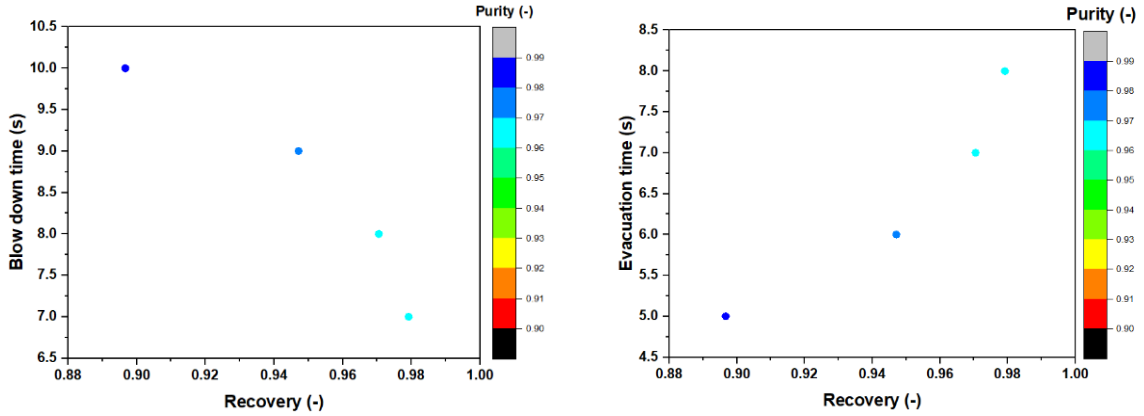

According to the right panel of Figure 24, CO_2 recovery is enhanced when evacuation step is almost 8 seconds (as opposed to its original step time of 5 seconds). Longer evacuation time helps to achieve a slightly lower pressure by the end of evacuation step resulting in the removal (desorption) of more CO_2 from the bed. Considering the total duration of blow-down and evacuation steps cannot be longer than 15 seconds, this consequently means a shorter step time for blow-down (7 seconds as opposed to the 10 second step time used originally) which will impact CO_2 purity negatively (left panel). The overall picture is consistent with our understanding that purity and recovery of the system are two competing KPIs that cannot be improved simultaneously.

We have also analysed the impact of blow-down and evacuation step times on CO_2 mass hold-up in the reactor by looking at the variation of this variable with respect to different step-times for blow-down and evacuation steps as shown in Figure 25.

Figure 25. Variation of CO_2 mass hold-up with respect to duration of blow down and evacuation steps

Variation of CO_2 mass hold-up with respect to duration of blow down and evacuation steps

Here, CO_2 mass holdup is higher when evacuation step time is around 8 seconds which is correlated to the higher recovery value achieved at this step-time according to Figure 24.

Impacts of Bed Porosity on System's KPIs

We have extended our sensitivity analysis to investigate the impact of porosity and the amount of available active materials on system's KPIs. Higher porosity normally means a larger volumetric fraction of the bed is empty (less adsorbent material available) and lower bed porosity will have the opposite effect. Varying bed porosity

also affects pressure drop across the bed. We have examined performance of the system for 3 different bed porosities at a fixed cycle configuration. Results of this analysis are provided in Table 4 with a visual presentation of productivity figures shown in Figure 26. This analysis is MOF agnostic, meaning the observed trends are not dependent on the specific m-MOF used. Bed porosity was varied independently of the MOF type simply to demonstrate its impact on process performance.

Table 4. System's KPIs for Gen.1 reactor design at different bed porosities

Bed Porosity (-)	Mass of MOF (kg)	Pressure-drop (bar)	Purity (-)	Recovery (-)	Volumetric Productivity (kg/m3/h)	Gravimetric Productivity (kg/kgMOF/h)
0.2	748	0.213	0.87	0.85	135	0.135
0.4	561	0.018	0.87	0.96	152	0.203
0.6	374	0.003	0.92	0.91	145	0.290

From the results presented in Table 4, it is evident that 300% increase in bed porosity results in 50% reduction of adsorbent mass in the reactor! This, however, does not guarantee a monotonic increase of volumetric productivity. In contrast, since higher porosity essentially corresponds to a decrease in the amount of active material, gravimetric productivity monotonically increases within the porosity range investigated here as shown in Figure 26.

Figure 26. Impact of Gen.1 reactor porosity on productivity of the system

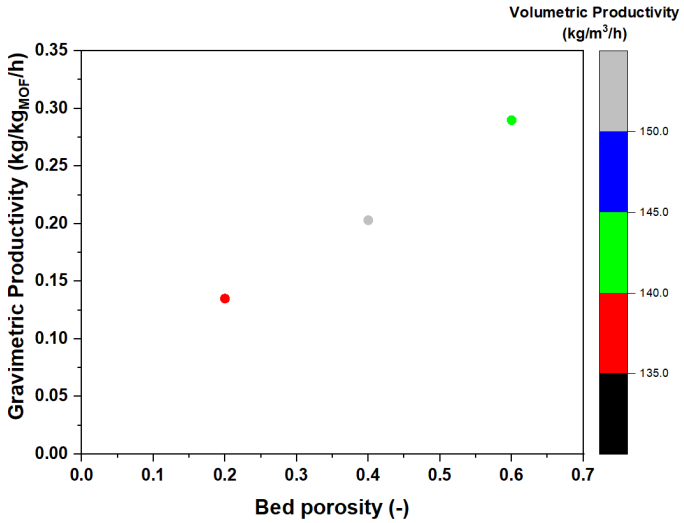

For the Gen.2 reactor design, the picture is distinctly different. In these reactors, bed porosity and mass of adsorbent can be varied by using different forms of structured materials (form factor). We have analysed system's performance for four different form factors for which the results are presented in Table 5.

Table 5. System's KPIs for Gen.2 reactor design at different reactor porosities

Form Factor	Bed Porosity (-)	Mass of MOF (kg)	Volumetric Productivity (kg/m3/h)	Gravimetric Productivity (kg/kgMOF/h)
Form 1	0.74	127	567.6	3.3
Form 2	0.74	98	491.0	3.8
Form 3	0.77	115	497.3	3.2
Form 4	0.78	109	529.3	3.7

Figure 27. Impact of bed porosity on system's productivity for Gen.1 and Gen.2 (various form factors) designs

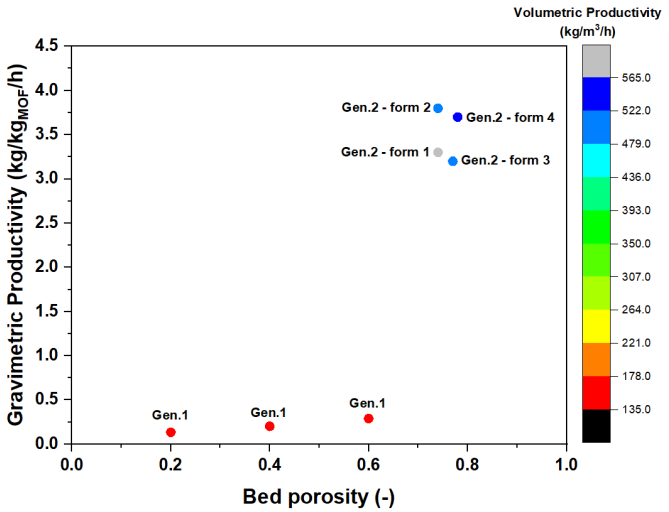

As shown in Figure 27, we can change the amount of adsorbent in the bed simply through changing the reactor porosity and form factor of our adsorbents.

4.2.5 – Summary

As part of 2nd work package of the CCUS project, we designed a scalable PVSA carbon capture system around the use of some of our top-performing m-MOFs. The new CO_2 capture system implements two different reactor designs namely Gen 1 and Gen 2. While the first generation of our system served as the basis of our design and a benchmark for future improvements, the 2nd generation was developed to meet the requirements of a commercial scale capture plant. Our modelling studies confirmed that the Gen.2 system outperforms its Gen.1 counterpart by a factor of 18 in terms of gravimetric productivity. The intensified PVSA process was shown to reach a capture capacity of 29 $\frac{\textbf{kte CO2}}{\textbf{te MOF.year}}$ at 98% purity and 90% recovery with 15% CO_2 concentration in the feed which is suitable for most transport and storage (T&S) applications and infrastructure.

4.3 WP3 – Test Rig Adaption and Experimentation

4.3.1 – Introduction

Work package 3 (WP3) of the CCUS project focuses on characterization and performance evaluation of top performing materials that were synthesized during

WP1. This work package allows the assessment of adsorption-desorption performance of the chosen materials through equilibrium uptake and dynamic column breakthrough (DCB) measurements. Moreover, WP3 provides critical information on structural stability of nominated adsorbents including their thermal, mechanical and chemical stabilities. Originally, the plan was to outsource this work package to Brunel and Swansea Universities. However, the construction of PVSA/PTSA rigs at these universities did not complete before the start of CCUS project. Consequently, WP3 was restructured and a new partnership with Cranfield University was formed. All changes were approved by DESNZ through a series of change requests submitted through the official channels. The updated scope of the work includes systematic and comprehensive characterization of IMM-16 and IMM-28 in their Gen 1 and Gen 2 forms.

The technical work carried out involved extensive measurement campaigns and data analysis. This section presents a summary of the key activities and outcomes to ensure clarity and focus.

4.3.2 – Experimental Set-ups

Three distinct classes of experiments have been conducted as part of WP3: a) experiments associated with measurement of competitive adsorption of gases, which were mainly carried out using the DCB technique; b) investigation of materials stability including their thermo-mechanical, and chemical stabilities; c) measurement of MOFs physical properties such as heat capacity and thermal conductivity. IMM-16 and IMM-28 were both tested in these measurements. Complete list of all experiments carried out as part of WP3 is presented in Table 6 and Table 7.

Table 6. Comprehensive list of DCB tests carried out for IMM-16 and 28 in their Gen. 1 and Gen. 2 forms. N_2 is the carrier gas in all tests.

Test Index	Test Title	MOF form/type	Particle Size (mm)	CO_2 Concentration (%)	Flowrate (ml/min)	Total Pressure (bar)	Temperature (˚C)	Relative Humidity (%)
1.1.	IMM-16_(2.8-3.35 mm)_15CO2_N2_200_1_25_0	Gen 1/IMM-16	2.8-3.35	15	200	1	25	0
1.2.	IMM-16_(2.8-3.35 mm)_15CO2_N2_400_1_25_0	Gen 1/IMM-16	2.8-3.35	15	400	1	25	0
1.3.	IMM-16_(2.8-3.35 mm)_15CO2_N2_600_1_25_0	Gen 1/IMM-16	2.8-3.35	15	600	1	25	0
1.4.	IMM-16_(2.8-3.35 mm)_15CO2_N2_800_1_25_0	Gen 1/IMM-16	2.8-3.35	15	800	1	25	0
1.5.	IMM-16_(2.8-3.35 mm)_15CO2_N2_400_5_25_0	Gen 1/IMM-16	2.8-3.35	15	400	5	25	0
1.6.	IMM-16_(0.25-0.5 mm)_15CO2_N2_400_1_25_0	Gen 1/IMM-16	0.25-0.5	15	400	1	25	0

1.7.	IMM-16_(2.8-3.35 mm)_15CO2_N2_400_1_45_0	Gen 1/IMM-16	2.8-3.35	15	400	1	25	0
2.1.	IMM-28_(2.8-3.35 mm)_15CO2_N2_200_1_25_0	Gen 1/IMM-28	2.8-3.35	15	200	1	25	0
2.2.	IMM-28_(2.8-3.35 mm)_15CO2_N2_400_1_25_0	Gen 1/IMM-28	2.8-3.35	15	400	1	25	0
2.3.	IMM-28_(2.8-3.35 mm)_15CO2_N2_600_1_25_0	Gen 1/IMM-28	2.8-3.35	15	600	1	25	0
2.4.	IMM-28_(2.8-3.35 mm)_15CO2_N2_800_1_25_0	Gen 1/IMM-28	2.8-3.35	15	800	1	25	0
2.5.	IMM-28_(2.8-3.35 mm)_15CO2_N2_400_5_25_0	Gen 1/IMM-28	2.8-3.35	15	400	5	25	0
2.6.	IMM-28_(0.25-0.5 mm)_15CO2_N2_400_1_25_0	Gen 1/IMM-28	0.25-0.5	15	400	1	25	0
2.7.	IMM-28_(2.8-3.35 mm)_15CO2_N2_400_1_45_0	Gen 1/IMM-28	2.8-3.35	15	400	1	45	0

3.1.	IMM-16_15CO2_N2_200_1_25_0	Gen 2/IMM-16	---	15	200	1	25	0
3.2.	IMM-16_15CO2_N2_400_1_25_0	Gen 2/IMM-16	---	15	400	1	25	0
3.3.	IMM-16_15CO2_N2_600_1_25_0	Gen 2/IMM-16	---	15	600	1	25	0
3.4.	IMM-16_15CO2_N2_1000_1_25_0	Gen 2/IMM-16	---	15	1000	1	25	0
3.5.	IMM-16_30CO2_N2_400_1_25_0	Gen 2/IMM-16	---	30	400	1	25	0
3.6.	IMM-16_15CO2_N2_400_1_45_0	Gen 2/IMM-16	---	15	400	1	45	0
3.7.	IMM-16_15CO2_N2_400_1_65_0	Gen 2/IMM-16	---	15	400	1	65	0
3.8.	IMM-16_15CO2_N2_1000_1_85_25	Gen 2/IMM-16	---	15	1000	1	85	25

3.9.	IMM-16_15CO2_N2_1000_1_85_50	Gen 2/IMM-16	---	15	1000	1	85	50
3.10.	IMM-16_15CO2_N2_1000_1_85_95	Gen 2/IMM-16	---	15	1000	1	85	95
4.1.	IMM-28_15CO2_N2_200_1_25_0	Gen 2/IMM-28	---	15	200	1	25	0
4.2.	IMM-28_15CO2_N2_400_1_25_0	Gen 2/IMM-28	---	15	400	1	25	0
4.3.	IMM-28_15CO2_N2_600_1_25_0	Gen 2/IMM-28	---	15	600	1	25	0
4.4.	IMM-28_15CO2_N2_1000_1_25_0	Gen 2/IMM-28	---	15	1000	1	25	0
4.5.	IMM-28_30CO2_N2_400_1_25_0	Gen 2/IMM-28	---	30	400	1	25	0

4.6.	IMM-28_15CO2_N2_400_1_45_0	Gen 2/IMM-28	---	15	400	1	45	0
4.7.	IMM-28_15CO2_N2_400_1_65_0	Gen 2/IMM-28	---	15	400	1	65	0
4.8.	IMM-28_15CO2_N2_1000_1_85_10	Gen 2/IMM-28	---	15	1000	1	85	10
4.9.	IMM-28_15CO2_N2_1000_1_85_50	Gen 2/IMM-28	---	15	1000	1	85	50
4.10.	IMM-28_15CO2_N2_1000_1_85_95	Gen 2/IMM-28	---	15	1000	1	85	95

In Table 6, each experiment is listed with a unique identifier (Index Number) and a Test Title with the latter having the following format:

Material name_CO_2 mole fraction_carrier gas_flowrate_pressure_temperature_relative humidity

For example: IMM-28_15CO2_N2_400_1_65_0 refers to an experiment carried out on IMM-28 with 15% CO_2 concentration in the feed and with N_2 as carrier gas at 400 l/min flowrate, 1 bar pressure, 65 degree Celsius temperature, and 0% relative humidity.

Table 7 Overview of material stability and physical property measurements

Test Index	Test Title	MOF Form/Type	Task Description
5.1.	Thermogravimetric Analysis (TGA)	Gen 1/IMM-16, IMM-28	Thermal and Cyclic Adsorption-Desorption Stability
5.2.	Attrition by Fluidization	Gen 1/IMM-16, IMM-28	Mechanical Stability
5.3.	Accelerated Ageing Test	Gen 1/IMM-28	Thermal and Mechanical Stability
5.4.	Differential Scanning Calorimetry (DSC)	Gen 1/IMM-16, IMM-28	Heat Capacity Measurement
5.5.	Laser Flash Analysis	Gen 1/IMM-16	Thermal Conductivity Measurement

Dynamic column breakthrough (DCB) measurements

Two different experimental set-ups were developed to carry out DCB experiments on Gen.1 and Gen. 2 reactors as shown in Figure 28 to Figure 31.

Figure 28. Experimental DCB set-up built with a Gen. 1 reactor

Figure 29. P&ID of the DCB set-up with a Gen. 1 reactor

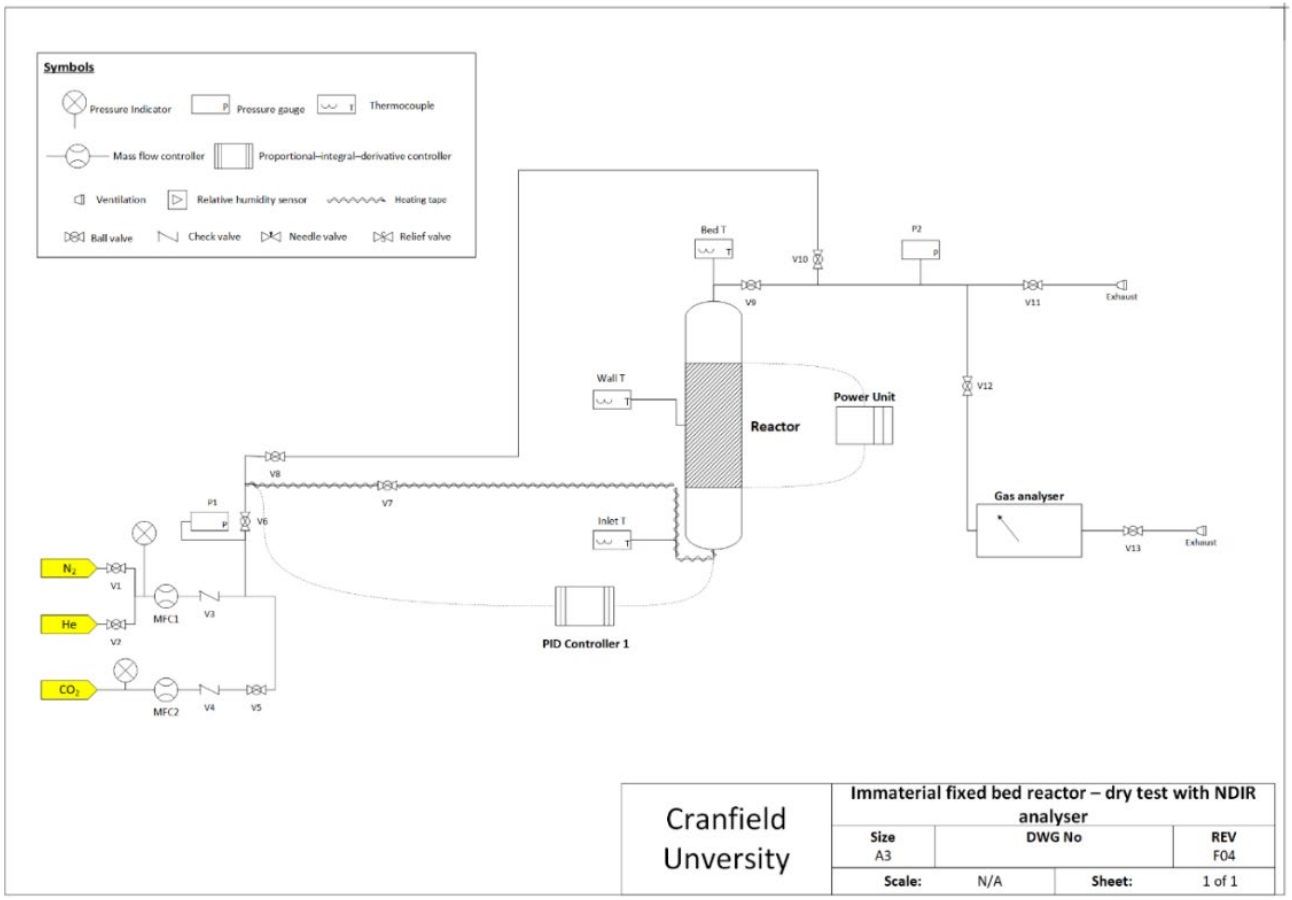

Figure 30. Experimental DCB set-up built with a Gen. 2 reactor

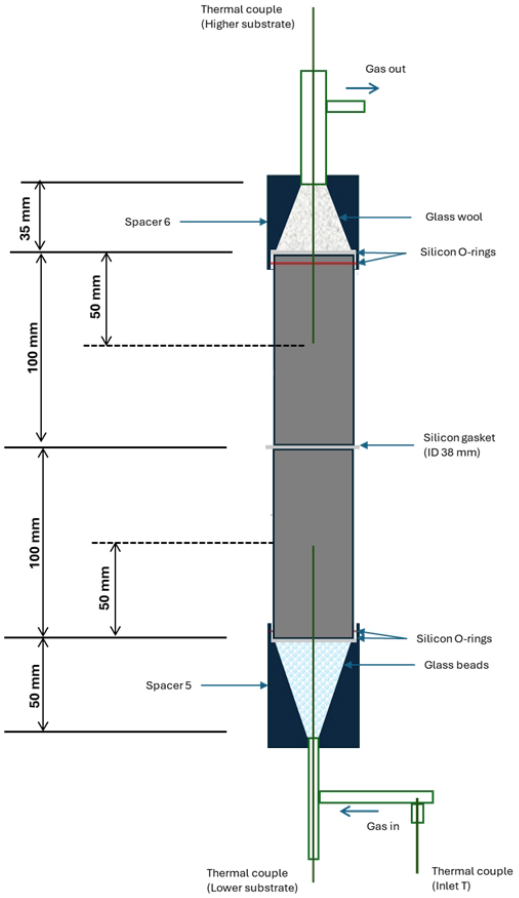

Figure 31. P&ID of the DCB set-up with a Gen. 2 reactor

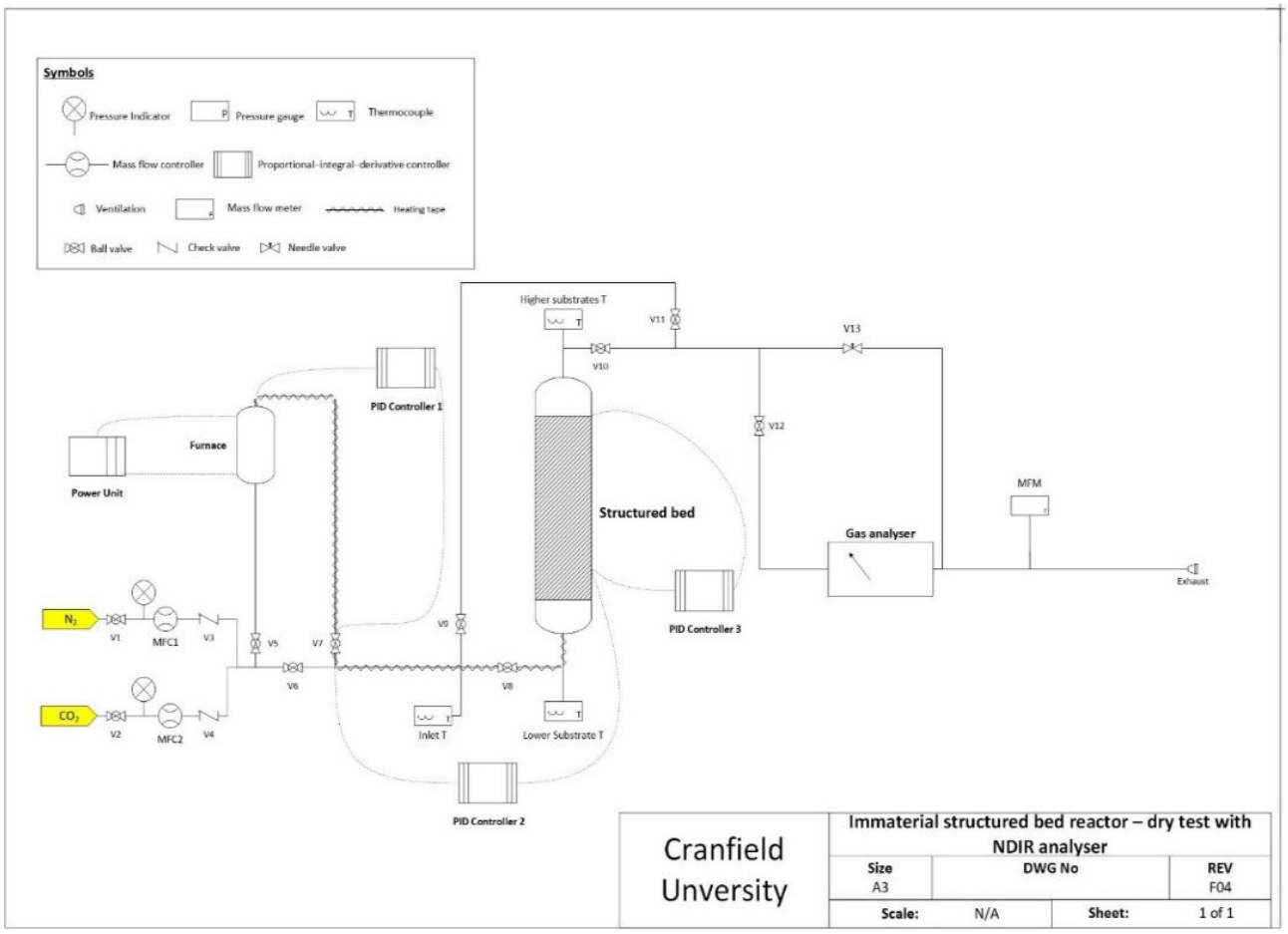

The DCB setup consists of a reactor loaded with either Gen. 1 or Gen. 2, adsorbent, where a gas mixture is continuously flowed into the bed while concentration of each gas component is monitored at the outlet. This is used to study competitive adsorption dynamic under various conditions. The gas mixture was prepared by blending CO_2 with a carrier gas (typically N_2 or He), using two mass flow controllers (MFCs) to precisely regulate individual flow rates. The total flow was introduced to the reactor inlet, where the feed conditions, e.g. feed flowrate, feed pressure, feed temperature, feed CO_2 concentration, and feed relative humidity, were systematically varied during the experiments.

Prior to each breakthrough test, the MOF bed was activated using a dedicated heating system capable of preheating the gas stream before entry into the reactor. Activation was carried out under a flow of dry gas, i.e. N_2 or He, at elevated temperatures to ensure removal of residual moisture and adsorbed CO_2. Once activated, the reactor was cooled to the desired test temperature before introducing the wet or dry feed.

The outlet gas from the reactor was routed to a CO_2 analyser, which continuously monitored the effluent concentration over time, enabling breakthrough curves to be recorded. These curves were then used to quantify the dynamic adsorption capacity

and analyse the impacts of process parameters on performance of Gen. 1 and Gen. 2 materials.

Special care was taken to minimize dead volumes and ensure uniform gas distribution across the bed. Challenges encountered during the setup and testing included maintaining consistent humidity levels at elevated temperatures, as well as thermal management of the reactor to avoid temperature gradients during activation and operation.

Material Stability Experiments

Thermogravimetric analysis (TGA)

We have employed TGA to investigate thermal stability and cyclic CO_2 capacity of our MOFs. By analysing mass changes of the MOF sample during heating and cooling cycles, we can obtain valuable information about their thermal decomposition patterns and structural stability. These data are crucial for understanding the temperature range within which our MOFs maintain their structural integrity. Additionally, TGA was used to assess the reversibility and performance of MOFs in CO_2 adsorption-desorption cycles.

Figure 32. Photographic image of the thermogravimetric analyser 8000 (Perkin Elmer).

Attrition by Fluidization

Attrition by Fluidization test was used to assess stability and resistance of adsorbent materials against mechanical degradation that can happen in fluidized reactors. Here, adsorbents are fluidized at different velocities of the feed gas and particle size distribution (PSD) of collected samples are measured afterwards. Analysis of the PSD data will tell us if pellets have been crumbled during the fluidization process.

Accelerated Ageing Test (AAT)

Accelerated ageing test is a crucial method employed to evaluate the long-term durability and performance of MOFs when exposed to specific operating conditions.

Here, the primary goal is to simulate the conditions to which the material is exposed. By exposing the MOF to these conditions in an accelerated manner, potential degradation or changes in adsorption capacity of MOFs can be assessed over a shorter period.

In our AAT tests, adsorbents were exposed to a simulated gas mixture with a composition similar to those of typical flue gas for duration of 2 weeks. After the test, CO_2 uptake of the adsorbents was measured in a DCB experiment and the results were compared against the original sample before any exposure test. The MOF was found to be stable under the test conditions considering there is no observable difference between the breakthrough curves before and after the exposure test.

Physical Properties Measurements

Differential Scanning Calorimetry (DSC)

We employed modulated differential scanning calorimetry using a thermal analysis (TA) instrument calorimeter to calculate specific heat capacity of our MOFs. This property is of particular importance in swing adsorption systems as it can control temperature fluctuations of the reactor during adsorption and desorption processes.

Thermal Conductivity Measurement

We employed the Laser Flash Analysis (LFA) using a TA Instrument model DLF 1200A to measure thermal conductivity of our MOFs. Thermal conductivity of an adsorbent plays a critical role in dissipation of thermal energy through the reactor potentially impacting adsorption/desorption uptake and kinetic of the process.

4.3.3 – Summary

Work package 3 of the CCUS project allowed extensive characterization of two of Immaterial's top performing m-MOFs (IMM-16 and IMM-28). As part of the work carried out during this work package, two different DCB rigs were developed and commissioned which were dedicated to testing of our Gen 1 and Gen 2 reactor designs. Suitability of each rig was carefully tested prior to the start of experiments and any necessary improvements were implemented. The actual experiments were divided into 3 categories: 1) breakthrough measurements, 2) aging and stability tests, 3) physical properties measurements.

As part of the above 3 categories, we tested sub-atmospheric and high-pressure uptake and kinetic of CO_2 adsorption process at different conditions of the feed including feed temperature, flowrate, composition, and relative humidity. We also examined, thermal, mechanical, and chemical stabilities of our Gen 1 MOFs. Key physical properties such as heat capacity and thermal conductivity of the adsorbents were also measured.

Key information obtained from WP3 was then used to validate and refine the models developed in WP2. The above experiments provided critical insights into the ways that key performance indicators (purity, recovery, productivity, etc.) of our PVSA process can be further improved.

We believe the valuable data obtained during WP3 will benefit Immaterial's system and material development efforts that will continue beyond the end of CCUS project.

5. Project Management

5.1 – Introduction

Immaterial utilized a tailored PRINCE2 methodology, drawing on insights from previous UKRI and EU-funded collaborative projects. This approach ensured structured communication and decision-making while allowing for flexibility in response to project developments.

A project team was formed, consisting of Immaterial's CTO, Project Manager, Technology Team Leads, and the Finance Director. The team held weekly meetings to review project progress and assess risks. Additionally, a monthly review meeting was held with the Project Monitoring Officer and the DESNZ Programme and Project Managers.

The Project Manager established a live Gantt chart and risk register to track any deviations from the plan and implement corrective actions as necessary. The project was completed on schedule and met the standards required by DESNZ.

5.2 – Project Completion Report

5.2.1 – Gantt Chart

		23												24												25	
		F	M	A	M	J	J	A	S	O	N	D	J	F	M	A	M	J	J	A	S	O	N	D	J	F	
Monolithic MOFs for CCUS		**Q1**			**Q2**			**Q3**			**Q4**			**Q5**			**Q6**			**Q7**			**Q8**			**Q9**	
		1	**2**	**3**	**4**	**5**	**6**	**7**	**8**	**9**	**10**	**11**	**12**	**13**	**14**	**15**	**16**	**17**	**18**	**19**	**20**	**21**	**22**	**23**	**24**	**25**	
WP1	**Material selection and optimisation**						**M1**				**M2**								**M3**								
1.1	Gen 1 & 2 materials identification & synthesis																										
1.2	Gen 1 & 2 synthesis optimisation																										
1.3	Monolith morphology optimisation								D1.1																		
1.4	Development of a MOF-based structured adsorbent																										
1.5	Robustness and stability optimisation														D1.2												
WP2	**Design of a PVSA/PTSA process model and heat exchanger**																						**M4,5**				
2.1	Development of the process model											D2.1															
2.2	Dynamic bed behaviour for monoliths											~~D2.2~~															
2.3	Model development for structured adsorbents														D2.3												
2.4	Dynamic bed behaviour for structured adsorbents																		D2.4								
2.5	Sensitivity analysis																					D2.5					
WP3	**Test rig adaptation and experimentation** *(subcontracted)*							**M6**																			
3.1	Conventional experiments for gen 1/2 monoliths										D3.1																
3.2	Design of experiments																										
3.3	Test rig adaptation																										
3.4	Test rig experimentation																									D3.2	
WP4	**Commercialisation & IP Strategy**																									**M7**	
4.1	Customer engagement and dissemination																								D4.1		
4.2	Implement IP strategy and apply for patent and other IP as required																										
WP5	**Project management**																									**M8**	
5.1	Kick off	D5.1																									
5.2	Internal communication & project management																										
5.3	Maintain live project documents																										
5.4	Monitoring of issues and risks																										
5.5	Monthly review meeting																									D5.2	

5.2.2 – Project Deliverables

WP#	Deliverable Title	Baseline Due Date	Updated Due Date with CR
1	D1.1 - Material optimisation report	30/11/2023	30/09/2023
1	D1.2 - Generation of structured adsorbents	31/03/2024	31/03/2024
2	D2.1 - Design of a VPSA Process Model	31/12/2023	31/12/2023
2	D2.2 - COMSOL model (heat exchanger)	31/12/2023	Removed
2	D2.3 - Model Development for Structured Adsorbents	31/03/2024	31/03/2024
2	D2.4 - Dynamic bed behaviour for structured adsorbents	30/06/2024	28/07/2024
2	D2.5 - Sensitivity Analysis of the DR-PVSA Process	30/09/2024	30/10/2024
3	D3.1 - Conventional Experiments for Gen 1&2 Monoliths	31/10/2023	31/10/2023
3	D3.2 - Test Rig Adaptation and Experimentation	30/06/2024	31/01/2025
4	D4.1 – Exploitation Plan	31/01/2025	31/01/2025
5	D5.1 - Project kick-off documentation	20/03/2023	20/03/2023
5	D5.2 – Final Project Report	31/01/2025	31/03/2025

5.2.3 – Communication Management

Project Team includes Immaterial CTO – Owen Garrigan, Project Manager – Jialin Tang, Work Package Leaders – Ceren Camur (WP1), Amir Farmahini (WP2 & WP3), Robin Gillham (WP4), Immaterial Finance Director – Peter Logsdon.

External Project Stakeholders includes Project Monitoring Officer - Andrew Proud, DESNZ CCUS Innovation Project Manager - Laura Milne, DESNZ CCUS Innovation Programme Manager – John Gordon.

Communication	Attendees	Frequency	Goal
Project Status Report	Project Team	Weekly	Review project progress and risks.
Project Review Meeting	All project stakeholders	Monthly	Present project results, gather feedback and discuss next steps.

6. Benefits and Dissemination Activities

Prior to commencing this project, Immaterial's expectation of the market requirements for point-source CO_2 capture for high CO_2 concentration to be 15-50% and medium CO_2 concentration to be 3-15%. However, during our market research and customer engagement activities we have gained a clearer understanding of flue gas compositions for each sector and as a result revised our ranges to suit our findings. The new ranges used are as follows: Low CO2 (3-5%) and High CO_2 (>10%). The low CO_2 range is specifically suited for natural gas power plants and the High CO_2 range covers Cement, Steel, Chemicals, Energy from Waste (EfW).

The primary objective of this project was to produce new materials for carbon capture and integrate them into modified Swing Adsorption systems. The combination of newly developed m-MOF materials and system design integration increases the volumetric capacity resulting in more CO_2 molecules being adsorbed within our materials, whilst also improving the systems operating efficiency. These outcomes allow Immaterial to offer significant advantages over both powdered MOF and amine technologies. By increasing the capture capability of our materials, it allows the system footprint to be reduced resulting in a lower capital expenditure and smaller operational expenditure.

During this project Immaterial have evaluated the techno-economic impact of our m-MOF materials and system designs when compared to the incumbent amine technology.

Immaterial's engagement with the target sectors have had positive outcomes. For a low concentration CO_2 European customer, we secured a purchase order and completed a techno-economic report which allowed us to understand the significant financial benefits that Immaterial's m-MOF material and system designs could provide to their decarbonisation targets. Immaterial has also been in discussions with another European low CO_2 emitter about a feasibility study and have been accepted onto their approve vendor list in preparation of a purchase order. Immaterial envisage the feasibility study to be completed by the end of Q2 2025.

For high CO_2 emissions Immaterial are engaged with a pipeline of multi-nationals for all sectors and have completed a feasibility study for a power generation company with a view to progression to a pilot demonstration on one of their sites. Immaterial are also in advanced discussions for feasibility studies with Cement and EfW companies.

Immaterial has also received various flue gas compositions across all target sectors which has allowed Immaterial to review the range of flue gas compositions to ensure compatibility to the m-MOF materials.

7. Lessons Learnt and Barriers

8.1 Overview

The project aimed to enhance Immaterial's carbon capture development work, focusing on system design capabilities. While the project faced delays, it exceeded expectations in quality and scope, providing a robust foundation for future development.

Project Delivery:

Timeliness: The project did not meet its original timeline due to delays associated with work conducted by Cranfield University and Change requests were submitted to extend the timeline.

Quality and Scope: Despite delays, the project surpassed expectations in quality and scope, significantly enhancing Immaterial's system design capabilities and market competitiveness.

Impactful Events:

Subcontractor Change: The change of subcontractor and the need to repeat some experiments by Cranfield caused delays.

Paperwork Delays: Initial paperwork with DESNZ led to a late start.

Approval Delays: The change request to switch subcontractors took longer than anticipated to be approved.

Success Factors:

Weekly Review Meetings: Regular meetings helped assess progress and plan actions when deviations occurred.

Cranfield University Engagement: Full engagement with Cranfield University, which showed flexibility in agreeing to scope changes based on ongoing results.

MO’s Support: Timely feedback, thorough review of technical reports, and guidance during change requests and financial claims were invaluable.

Areas for Improvement:

Proposal Preparation: Allocate more time during the proposal preparation stage to ensure resource and budget planning.

Project Handover: Establish a project handover checklist and implement a thorough review process before the departure of project stakeholders.

Data Management: Develop a data management plan during the project initiation stage to avoid issues with file location and version history.

Future Actions:

Proposal Preparation: Allocate more time for proposal preparation and leverage strong industry and academic connections.

Weekly Catch-ups: Maintain regular weekly catch-ups to discuss future opportunities and project progress.

Project Initiation: Apart from communication management, risk management, set up data management plan and project handover checklist during project initiation stages.

8.2 Conclusion

Despite its delays, the project has been a significant success in terms of quality and scope. By implementing the recommended improvements and actions, Immaterial

can enhance future project delivery, ensuring timely and efficient execution while maintaining high standards of quality and scope.

8. Project Impact and Route to Commercialization

As part of the commercial activities Immaterial have developed a target pipeline for the identified sectors/applications. Engagement has been undertaken with potential customers.

These discussions have resulted in various NDA's being agreed and signed. This has led to detailed technical discussions, Feasibility / Techno-Economic Study quotations and receiving Purchase Orders. As described in the section above (Benefits and Dissemination Activities) Immaterial have now completed Studies for both High and Low concentration CO_2 applications.

This project has allowed Immaterial to develop new m-MOF materials and system designs, generate IP protection, positioning us to be able to take advantage of the follow-on DESNZ CCUS call, and allow Immaterial to progress to the manufacture of a pilot demonstration unit. Immaterial has engaged a company within our target sectors, who have expressed a desire to work with us on the next DESNZ call to prove the technology in a pilot demonstration on one of their sites. This is an important step and Immaterial are eager to understand the timings for the next CCUS grant call from DESNZ. This next step is imperative in the commercialisation roadmap for the technology as it enables Immaterial to demonstrate the technology in an industrial setting to prove the materials and system design.

A further outcome during this project was to create a 5-year exploitation plan for the commercialisation of the technology. The plan reflects a clear roadmap through securing purchase orders for initial technology demonstration in Year 1, allowing for full design and build of the system with commissioning / operation in Year 2-3. The technology demonstration will provide operating performance data for the materials and system design. This information will allow Immaterial to incorporate any learning and modifications to the designs whilst providing justification to the emitter to secure funding and progress to a large-scale pilot demonstration unit. Years 4-5 will allow for the larger system design, build and commissioning to take place. This larger-scale pilot will provide the emitter with full techno-economics of the system, including scalability of both system design and material manufacture. These stages are designed to address potential hurdles envisaged by customers to progress to industrial-scale carbon capture.

9. IP Management

The disruptive nature of Immaterial's technology will provide our customers with significant financial benefits in both CAPEX and OPEX savings. Therefore, the Intellectual Property (IP) protection of the materials and designs are critical to Immaterial's uniqueness and company valuation.

Immaterial has a proactive IP strategy focussing on m-MOF chemistries, manufacturing processes, and carbon capture applications.

Immaterial has carried out an extensive landscaping of the IP in the context of carbon capture in conjunction with an external search specialist (J&B Partners) to assess freedom to operate for the solutions being developed by Immaterial.

Due to the disruptive nature of the technology Immaterial have spent considerable time in understanding and agreeing strict long-term NDA's, Agreements and T&Cs with our customers to maximise protection of our Intellectual Property Rights (IPR).

If you need a version of this document in a more accessible format, please email alt.formats@energysecurity.gov.uk. Please tell us what format you need. It will help us if you say what assistive technology you use.